Chinese Journal of
POLYMER SCIENCE

REVIEW

• 2026 Rising Scholars •

https://doi.org/10.1007/s10118-026-3635-4
Chinese J. Polym. Sci. **2026**, *44*, 2086–2111

Advancing the Thin-film Mechanics of Conjugated Polymers: Characterization, Modulation, and Innovation

Jin-Tao Feng and Long Ye*

School of Materials Science and Engineering, State key Laboratory of Advanced Materials for Intelligent Sensing, Tianjin Key Laboratory of Molecular Optoelectronic Sciences, Key Laboratory of Organic Integrated Circuits, Ministry of Education, Collaborative Innovation Center of Chemical Science and Engineering, Tianjin University, Tianjin 300072 China

Abstract Conjugated polymer thin films are key functional layers in flexible and wearable devices, where mechanical behavior directly influences device performance and stability. However, accurate mechanical characterization remains challenging due to their nanoscale thickness and brittleness. This review aims to offer a holistic view on thin-film mechanics of conjugated polymers and systematically summarizes static and dynamic mechanical characterization methods for conjugated polymer thin films, spanning bulk materials, substrate-supported ultrathin films, and freestanding ultrathin films, and elucidates the measurement principles and key features of each technique. By integrating reported experimental results, we identify multiple factors affecting thin-film mechanical behavior. Finally, an outlook is presented in which, guided by device-level mechanical requirements, the mechanical behavior of polymer optoelectronic thin films is designed and regulated through multiple strategies, and comprehensively evaluated using complementary mechanical characterization approaches, enabling subsequent optimization based on the measured mechanical response.

Keywords Conjugated polymers; Stretchable electronics; Organic electronics; Polymer films; Mechanical properties

Citation: Feng, J. T.; Ye, L. Advancing the thin-film mechanics of conjugated polymers: characterization, modulation, and innovation. *Chinese J. Polym. Sci.* **2026**, *44*, 2086–2111.

1 INTRODUCTION

The mechanical properties of organic and polymeric semiconductors have emerged as critical frontiers in materials science, determining the feasibility and durability of next-generation flexible and wearable electronics. Conjugated polymer thin films are fundamental to the advancement of this modern field because they uniquely combine solution processability, tunable optoelectronic function, and intrinsic mechanical compliance.[1–6] Their softness and compatibility with low-temperature fabrication enable soft electronic devices to be bent, folded, or stretched while remaining functional.[7–11] Conse-

* Corresponding author, E-mail: yelong@tju.edu.cn
Received December 29, 2025; Accepted February 26, 2026; Published online May 7, 2026

quently, these materials are increasingly pivotal across a spectrum of emerging technologies, from personalized healthcare to soft robotics and seamless human-machine interfaces. These polymer films function as active or charge-transport layers across diverse device classes. Organic photovoltaics (OPVs) often form a photoactive medium in lightweight, bendable, and stretchable solar cells that are used for self-powered wearables, epidermal energy harvesters, and portable power modules.[12–21] Organic photodetectors (OPDs) facilitates health monitoring, biomedical imaging, motion sensing, and low-power optical communication systems.[22–25] For organic light-emitting diodes (OLEDs), mechanically robust emissive layers underpin flexible, rollable, and conformable displays, as well as adaptable lighting panels.[26–31] In organic field-effect transistors (OFETs), conjugated polymer films enable flexible circuitry, chemical and gas sensors, electronic skins, and soft-robotic interfaces.[32–36] The breadth of these applications underscores a fundamental material challenge: conjugated polymer films must simultaneously deliver high optoelectronic performance and durable mechanical behavior under operational deformation (Fig. 1). Therefore, achieving optimal stretchability, fracture toughness, and long-term mechanical reliability is no longer a secondary consideration but a critical prerequisite for the successful development of next-generation wearable and deformable optoelectronics.

Despite these promising attributes, the majority of current research remains narrowly focused on improving conventional optoelectronic performance metrics such as power conversion efficiency, charge carrier mobility, and device stability. Although these parameters are undeniably important, the mechanical stability of conjugated polymer thin films is equally crucial, particularly for devices intended for flexible and stretchable applications. Long-term operation in real-world environments inevitably subjects these devices to cyclic mechanical strain, bending, and deformation; in such scenarios, inadequate mechanical durability frequently emerges as the primary mode of failure. Consequently, a comprehensive understanding and accurate characterization of the intrinsic mechanical properties of conjugated polymer thin films are essential to bridge the gap between laboratory-scale device demonstrations and the development of reliable, commercially viable flexible electronics.

Conventional mechanical testing methods designed for bulk materials (*e.g.*, millimeter-scale specimens) often fail to capture the unique physics of confined, anisotropic polymer systems at device-relevant thicknesses (typically <200 nm). This limitation stems from fundamental issues such as substrate constraints, interfacial adhesion artifacts, and the profound influence of processing history on the non-equilibrium film morphology. Consequently, accurate measurement and fundamental understanding of properties such as the intrinsic modulus and fracture energy in the freestanding or near-freestanding state remains a central challenge. In recent years, new mechanical characterization methodologies have evolved substantially, progressing from traditional bulk material tests[37,38] to a sophisticated suite of methods designed explicitly for nanoscale thin films. This evolution encompasses methods such as surface buckling metrology and elastomer-supported tensile methods (the most popular is the film-on-elastomer method (FOE)),[39–43] tensile assays on liquid substrates such as the film-on-water (FOW) approach,[44–47] and specialized platforms designed for the direct tensile characterization of freestanding ultrathin films.[48–56] Parallel advancements have also enabled the adaptation of dynamic mechanical analysis (DMA) for both bulk polymers and confined thin films,[57–63] providing crucial insights into viscoelastic behavior and glass transition phenomena. Collectively, these recent methodological innovations have significantly enhanced our ability to probe the intrinsic mechanical responses of conjugated polymer thin films with unprecedented precision, and importantly, with direct relevance to their operational behavior in flexible and stretchable devices.

Motivated by these critical needs, this review aims to pro-

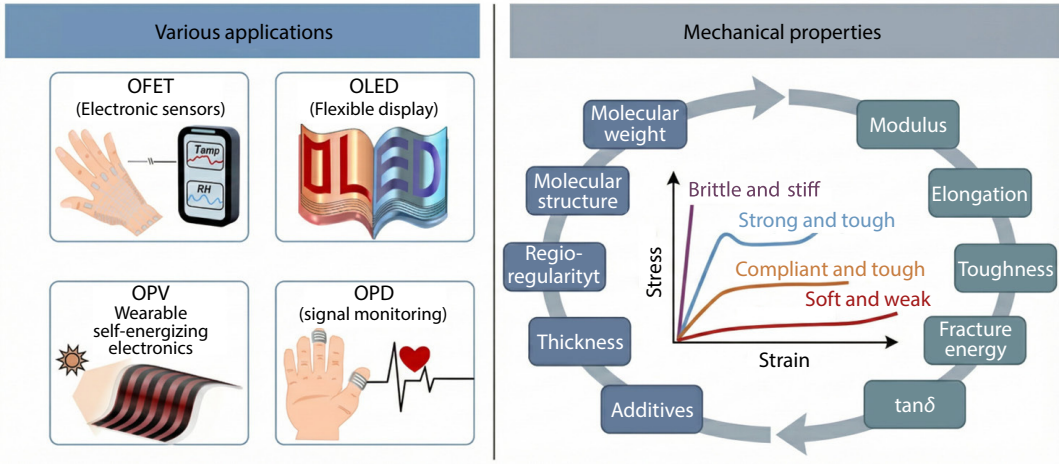

Fig. 1 A holistic view of conjugated polymer thin film mechanics. The schematic illustrates the integrated relationship between molecular design, material properties, mechanical performance, and stretchable optoelectronic applications. It summarizes how intrinsic material factors (molecular structure, molecular weight, regioregularity) and processing parameters (film thickness, additives) collectively govern key mechanical metrics, including elastic modulus, elongation at break, toughness, and fracture energy. These properties span distinct material regimes, ranging from brittle and stiff to compliant and tough, which directly influence the reliability and function of flexible organic electronic devices such as OPVs, OPDs, OLEDs, and OFETs.

https://doi.org/10.1007/s10118-026-3635-4

vide a holistic perspective on conjugated polymer thin-film mechanics, connecting fundamental material properties to the performance demands of stretchable optoelectronics. We systematically summarize the recent evolution of precise mechanical characterization methods and the principal strategies for modulating the mechanical properties of these thin films. The following sections critically review this methodological progress, analyze the fundamental polymer physics insights afforded by each technique, and provide a concise overview of the key strategies for mechanical optimization. By delineating representative material systems, establishing structure-mechanical property relationships, and evaluating practical modulation routes, including molecular design, processing, blending, and additive engineering, we aim to offer a coherent framework for bridging film structure, mechanical behavior, and device functionality. Ultimately, this integrated perspective is intended to guide the rational design of reliable, high-performance, and stretchable optoelectronic materials.

2 FOUNDATIONS OF THIN-FILM MECHANICS IN CONJUGATED POLYMER THIN FILMS

2.1 Structural Origins of Mechanical Behavior

The mechanical behavior of conjugated polymers used in optoelectronic thin films arises directly from their characteristic molecular architectures and multiscale morphologies. At the molecular level, these materials consist of rigid, π-conjugated backbones that impart electronic functionality but inherently limit chain mobility and extensibility,[64] together with flexible alkyl side chains that partially counteract backbone stiffness by increasing the free volume and enhancing local conformational flexibility.[65,66] This interplay establishes a fundamental balance between the stiffness and ductility, which governs the macroscopic response of the films.

Beyond single-molecule characteristics, conjugated polymers organize into hierarchical morphologies spanning multiple length scales, including semicrystalline fibrillar networks, separated phase or donor-acceptor domains, and intervening amorphous interphases. The spatial arrangement and connectivity of these morphological features have a decisive influence on the macroscopic mechanical behavior. Ordered or crystalline regions generally enhance stiffness and strength by promoting efficient intermolecular packing; however, they also tend to localize stress and reduce fracture strain.[67–69] In contrast, amorphous domains provide compliant regions that accommodate large deformations and dissipate mechanical energy through chain mobility and segmental relaxation. Consequently, key molecular and microstructural parameters such as intermolecular packing, degree of regioregularity, molecular weight and polydispersity, domain size and connectivity, and the presence of a secondary phase collectively govern the chain entanglement density, relaxation dynamics, and ultimately the dominant failure modes of conjugated polymer thin films.[70–74]

Processing and morphology introduce further complexity: solvent-driven orientation,[75–78] drying kinetics,[76,77] residual stress from film formation, and nanoconfinement,[79] all of which alter the local morphology and lead to thickness- or substrate-dependent mechanical responses. For these reasons, structural characterization, such as grazing incidence wide-angle X-ray scattering (GIWAXS), grazing-incidence small-angle X-ray scattering (GISAXS), X-ray diffraction (XRD), atomic force microscopy (AFM), transmission electron microscopy (TEM), and other relevant spectroscopies, should be accompanied by mechanical testing to interpret the measured modulus, yield behavior, toughness, and viscoelastic transitions in a physically meaningful way.

2.2 From Bulk to Thin-film Mechanics: Why New Methods are Essential

Traditional bulk mechanical tests, in particular uniaxial tensile tests, standard DMA on bulk specimens, and bulk fracture-toughness assays, have long provided reliable benchmarks such as Young's modulus, yield stress, elongation at break, fracture energy, and viscoelastic spectra for polymer engineering.[37,38] However, intrinsic and practical limitations render conventional mechanical tests unsuitable for characterizing optoelectronic polymer films at device-relevant thicknesses. Bulk specimens at millimeter to centimeter scales fail to reproduce the confinement effects, high surface-to-volume ratios, and thickness-dependent morphological gradients present in nanometer-scale films, resulting in size-dependent phenomena, such as nanoconfinement and surface-induced molecular ordering.[80] Mechanical responses governed by substrate constraints, interfacial adhesion, and stress transfer in supported device configurations are also absent in bulk measurements, and substrate interactions can stiffen or soften polymer films relative to bulk behavior.[81] In addition, solution processing and thermal annealing introduce anisotropy, thickness inhomogeneity, and residual stresses that lead to spatially heterogeneous mechanical behavior beyond the scope of bulk tests. Residual stress and constraint effects are well documented for thin film systems on rigid and compliant substrates.[82] Thin films exhibit deformation and failure modes that are distinct from those of bulk materials, including interfacial delamination, localized necking, and substrate-induced cracking, which are not captured by bulk fracture metrics. Such failure channels have been correlated with substrate constraints and processing history in brittle and ductile thin films.[83,84] Finally, thermomechanical properties such as the glass transition temperature and relaxation spectra can deviate substantially from bulk values, with T_g shifts and altered viscoelastic dynamics reported in supported polymer thin films, leading conventional DMA measurements to misrepresent device-relevant viscoelastic behavior.[85–88]

Because of these limitations, researchers have developed a series of thin-film-specific techniques designed to minimize or control substrate influence or operate in the low-force regime with high sensitivity and finally access both intrinsic and supported mechanical responses. Thin-film mechanical tests can be organized along two complementary axes: one is the degree of substrate constraint, which is from supported to freestanding, and the other is the measurement type, such as static *versus* dynamic. Overall, thin-film mechanical characterization methods can be broadly grouped into three categories (Fig. 2). Bulk testing applies uniaxial loading or oscillatory deformation to millimeter-scale specimens, yielding conventional metrics, such as modulus, strength, elongation at break, and viscoelastic transitions. However, these measurements do not reflect confinement or substrate effects in the

https://doi.org/10.1007/s10118-026-3635-4

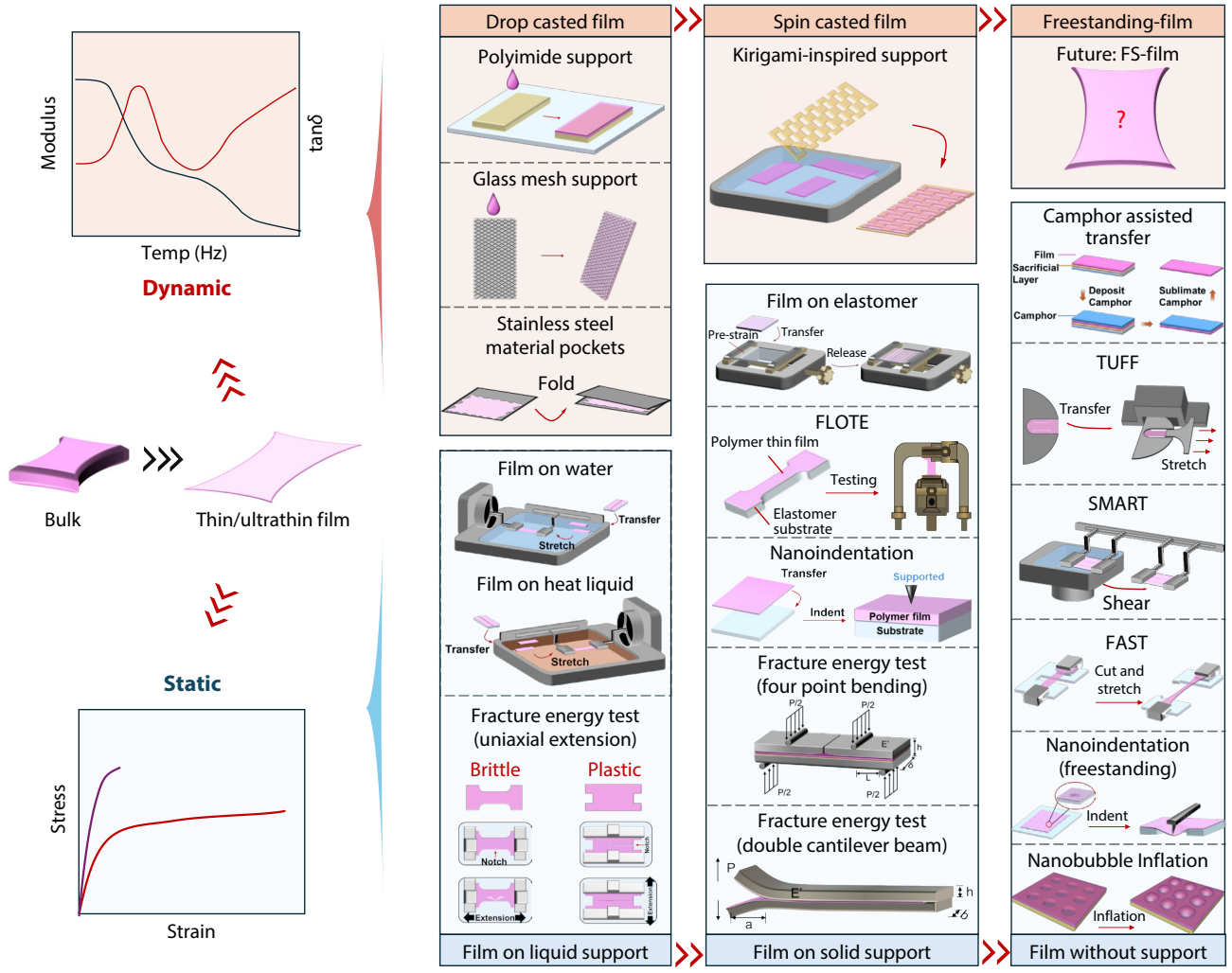

Fig. 2 Evolution and categorization of mechanical characterization methods for conjugated polymer thin films. The diagram illustrates the progression of techniques from dynamic to static testing, and from supported to freestanding configurations.

thin films. Supported film testing measures films while they remain on rigid, compliant, or liquid substrates, typically by imposing a local indentation, in-plane stretching, or substrate-induced deformation. These approaches are experimentally accessible and device-relevant; however, the measured response inherently includes contributions from the underlying support. In contrast, freestanding film testing evaluates suspended films through direct tensile loading, enabling the measurement of intrinsic mechanical properties, including true tensile modulus, intrinsic fracture behavior, and large strain ductility.

3 STATIC MECHANICAL CHARACTERIZATION METHODS FOR CONJUGATED POLYMER THIN FILMS

Static mechanical characterization emphasizes parameters such as the Young's modulus, yield strength, fracture strain, and toughness under quasi-static loading. The progression from supported to freestanding films aims to isolate intrinsic mechanics from substrate constraints, enabling better correlation with device performance in flexible optoelectronics and enhancing the understanding of how molecular structures translate to macroscopic performance. Below, we detail these methods sequentially, beginning with liquid-supported films for minimal constraints, advancing to solid supports for controlled testing, and culminating in freestanding techniques for ultimate accuracy.

3.1 Film on Liquid Support Methods

The film-on-liquid support approach represents one of the earliest and most effective strategies for approximating the substrate-free static mechanical testing of ultrathin polymer films. By floating the polymer film on a liquid surface, such as water, ionic liquids, or oils, at different temperatures, the extremely low shear modulus of the liquid, high surface tension, and low viscosity provide nearly constraint-free lateral support. This configuration dramatically suppressed the artificial stiffening and residual stress commonly imposed by solid substrates, thereby yielding mechanical parameters that closely approached the intrinsic values of the freestanding film. The key advantages of this method include an effective near-zero substrate modulus, thereby achieving a soft substrate limit and minimizing the substrate-induced mechanical constraints. In addition, the absence

of a solid-solid interface eliminates the adhesion inhomogeneity and associated stress concentrations that commonly arise at rigid supports. The method further offers straightforward sample preparation, making it compatible with a wide range of solution-processable conjugated polymers, as well as small organic molecules. Finally, by selecting the appropriate liquid media, measurements can be readily performed over a broad and tunable temperature range.

3.1.1 Film on water

A typical protocol involves preparing the polymer film on a water-soluble sacrificial layer such as poly(styrenesulfonate) (PSS), transferring it onto the liquid bath, and then performing uniaxial or biaxial tensile testing with customized grippers or floating clamps while recording stress-strain curves in real time. The film-on-water (FOW) tensile testing technique was pioneered by Kim *et al.*, who initially applied it to characterize the mechanical properties of ultrathin gold films.[44] This method can be extended to a diverse array of ultrathin and two-dimensional materials, including graphene, ultrathin silicon, metal oxides, organic-inorganic hybrids, and biomembranes, all supported on a liquid surface. By leveraging the negligible shear modulus of water to minimize lateral constraints and substrate-induced artifacts inherent in solid supports, the FOW approach yields mechanical parameters that are substantially closer to the intrinsic freestanding response, thereby representing a significant advancement in the precise mechanical characterization of optoelectronic polymer thin films.[45,70–72,79,89–91]

A landmark demonstration of the utility of the FOW method is its application to compare bulk-heterojunction active layers in all-polymer OPVs. Kim *et al.*[70] directly compared systems based on fullerene acceptor PCBM versus polymeric acceptor P(NDI2HD-T). As shown in Fig. 3(a), while both systems achieved comparable photovoltaic efficiencies, the all-polymer blend exhibited a significantly higher elongation at break and greater toughness. This superior mechanical robustness translated directly into enhanced device durability, and after more than 100 bending cycles, all-polymer devices retained approximately 90% of their initial performance, whereas [6,6]-phenyl-C_{71}-butyric acid methyl ester (PCBM)-based devices suffered near-complete failure.[70] In a related study, the same group used FOW to demonstrate a critical trade-off in poly(3-hexylthiophene) (P3HT)-based systems, showing that higher regioregularity increases the elastic modulus and initial device efficiency, but simultaneously reduces fracture strain and long-term mechanical stability under deformation.[72] These studies collectively underscore how FOW tensile data can reveal fundamental structure-property relationships.

Beyond its utility in applied device analysis, the FOW platform has emerged as a powerful tool for uncovering fundamental polymer physics in confined geometries. Crosby *et al.* systematically investigated the nanoconfinement effects in ultrathin films,[45,79] while Gu *et al.* uncovered pronounced room-temperature viscoelasticity in conjugated polymers such as P3HT and poly(2,5-bis(2-decyltetradecyl)-3,6-di(thiophen-2-yl)diketopyrrolo[3,4-c]pyrrole-1,4-dione-*alt*-thienovinylthiophene (DPP-TVT) floating on water, attributing the exceptional ductility to glass-transition temperatures below

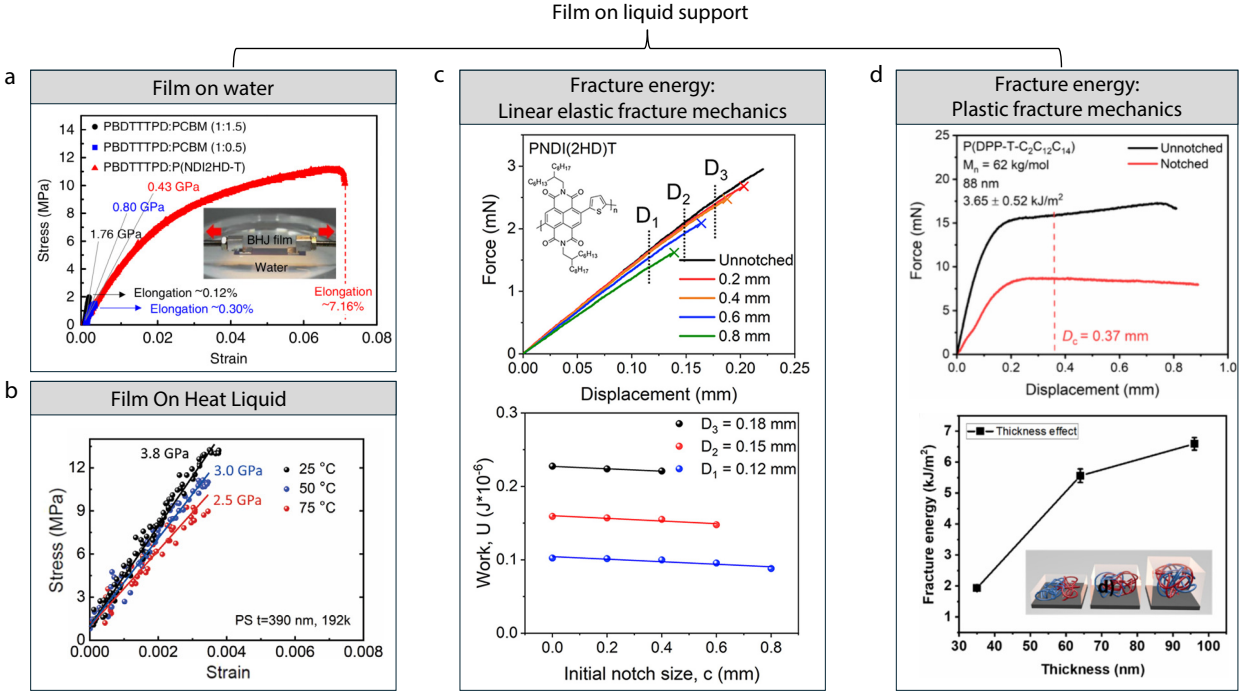

Fig. 3 Mechanical tensile testing methods for films on liquid supports. (a) Mechanical properties of bulk-heterojunction active layers based on fullerene PCBM versus polymeric acceptors P(NDI2HD-T) using FOW method (Reproduced with permission from Ref. [70]; Copyright (2015), Springer Nature). (b) Temperature-dependent mechanical characterization of PS thin films conducted using the film on heated liquid (FOHL) method (Reproduced with permission from Ref. [46]; Copyright (2024), John Wiley and Sons). (c) Fracture energy measurement within the elastic regime (Reproduced with permission from Ref. [47]; Copyright (2021), American Chemical Society) and (d) under the influence of plastic deformation for water-supported thin films (Reproduced with permission from Ref. [92]; Copyright (2025), American Chemical Society).

room temperature.[91] Together, these studies established the film-on-water method as a cornerstone technique for obtaining reliable, near-intrinsic mechanical properties that directly guide the development of robust, high-performance flexible optoelectronic devices.

3.1.2 Film on heat liquid

Kim *et al.* further extended the liquid-supported concept by introducing the film-on-hot-liquid (FOHL) technique, in which the polymer film is floated on a glycerol surface instead of water.[46] Glycerol was selected because of its excellent thermal stability, high surface tension, and full miscibility with water, enabling seamless transfer from an intermediate sacrificial layer. The experimental protocol closely mirrors FOW: the film is first prepared on a sacrificial layer such as Cu, transferred onto a specific liquid to etch the Cu layer, and then gently scooped onto preheated glycerol. Temperature-dependent tensile testing was subsequently performed by controlling the temperature of the glycerol bath. Using polystyrene as a model system, they demonstrated pronounced thickness-dependent softening; at elevated temperatures, thinner PS films exhibited a steeper drop in elastic modulus than their thicker counterparts (Fig. 3b). The FOHL method expands the accessible temperature window, which is typically from room temperature to above 100 °C while preserving the near-zero shear constraint of the liquid support, which provides a powerful platform for probing the thermomechanical response of optoelectronic polymers under processing- or operating-relevant thermal conditions that are inaccessible to conventional film-on-water measurements.

Furthermore, the film-on-liquid support approach can be adapted to simulate specialized operating environments, such as human sweat or saline conditions, by modifying the chemical composition of the liquid support. This flexibility allows researchers to evaluate the influence of chemical stressors on the interfacial stability and mechanical responses of polymers intended for epidermal applications.

3.1.3 Fracture energy test assisted by water

Gu's group developed a water-assisted fracture energy test for ultrathin polymer films using the Begley–Landes method.[47] (Fig. 3c) For brittle or linear-elastic films, a sharp pre-crack of a controlled length was introduced at the film edge using a laser cut. The film was then uniaxially stretched on water while recording the force–displacement response. Within the linear-elastic regime, the work required for crack propagation, *U(D)*, was obtained by integrating the area under the curve up to a selected displacement *D* prior to unstable crack growth. The fracture energy G_c was calculated as follows:

$$G_c = \frac{1}{t}\frac{dU}{dc}\Big|_D \quad (1)$$

where *t* is the film thickness and *c* is the crack length. By varying the initial crack length, a reliable G_c value was extracted from the slope of *U* versus *c*. For ductile polymers exhibiting significant plastic dissipation, the protocol was modified: a central crack spanning approximately half the film width was created, and the critical displacement D_c at the onset of the load drop while the progress of crack propagation was identified.[92] (Fig. 3d) Another pristine uncracked film was stretched to the same D_c, and the external work, $U(D_c)$, was measured. The plastic fracture energy is then determined as follows:

$$G_c = \frac{U(D_c)}{W \cdot t} \quad (2)$$

where *t* is the film thickness and *W* is the initial width of the uncracked film. Using this methodology, the authors systematically investigated the conjugated polymer DPP-TVT and revealed that the fracture energy decreases with decreasing film thickness from 100 nm to 30 nm, owing to reduced interchain interactions and a relative increase in intrachain contributions under nanoconfinement. A similar reduction was observed with decreasing molecular weight, which was rationalized through the viscosity-dependent chain entanglement density. This water-assisted fracture energy framework is a quantitative and versatile approach currently available for evaluating the cohesive toughness of brittle and ductile optoelectronic polymer thin films under conditions approaching the freestanding state.

3.2 Film on Solid Support Methods

Solid-supported film methods employ compliant substrates such as elastomers or thin laminated layers to provide controlled mechanical support for ultrathin optoelectronic polymer films during static testing. Unlike liquid supports, these solid configurations offer enhanced stability, repeatability, and compatibility with microscale instrumentation, enabling the precise measurement of parameters such as elastic modulus, crack onset strain, stiffness, and fracture energy. However, they introduce moderate interactions between the substrate and film, which must be accounted for in data analysis. The key methods, progressing from global tensile or compressive testing to localized probing and fracture assessment, are discussed below.

3.2.1 Film on elastomer

The film-on-elastomer (FOE) technique involves adhering the polymer film to an elastomeric substrate, which is typically PDMS, and derives mechanical properties from tensile or compressive deformation. This yields two critical parameters for optoelectronic active layers: the elastic modulus *E* and the crack onset strain *COS* (Fig. 4a). For modulus measurement, the FOE relies on buckling-based metrology, where sinusoidal wrinkles formed on the compressed film are analyzed to compute the tensile modulus. This approach has been successfully applied to the synthesis of various organic semiconductor polymers and small molecules. Whitesides *et al.* first reported buckling phenomena in metal films on PDMS substrates,[93] whereas Staffor extended the method to quantify the polymer film modulus.[40,41] Subsequent studies have widely adopted this approach for organic semiconductors.[65,67,89,94–98] The protocol begins with coating a water-soluble sacrificial layer on a glass substrate, followed by spin-coating the organic semiconductor film, which is then contacted with a strained elastomer ($\varepsilon \leq 5\%$) and immersed in water to dissolve the sacrificial layer, facilitating transfer. Upon releasing the strain to 0%, compressive stress induced wrinkles in the film. The buckling wavelength λ should be promptly measured to avoid time-dependent relaxation effects. The film modulus E_f was calculated from λ and the film thickness d_f using the following formula:

$$E_f = 3E_s\left(\frac{1-\nu_f^2}{1-\nu_s^2}\right)\left(\frac{\lambda}{2\pi d_f}\right) \quad (3)$$

where E_s is the substrate modulus and ν_f and ν_s are the Poisson's ratios of the film and substrate, respectively. The wavelength increased with higher E_f or d_f, enabling reliable modulus extrac-

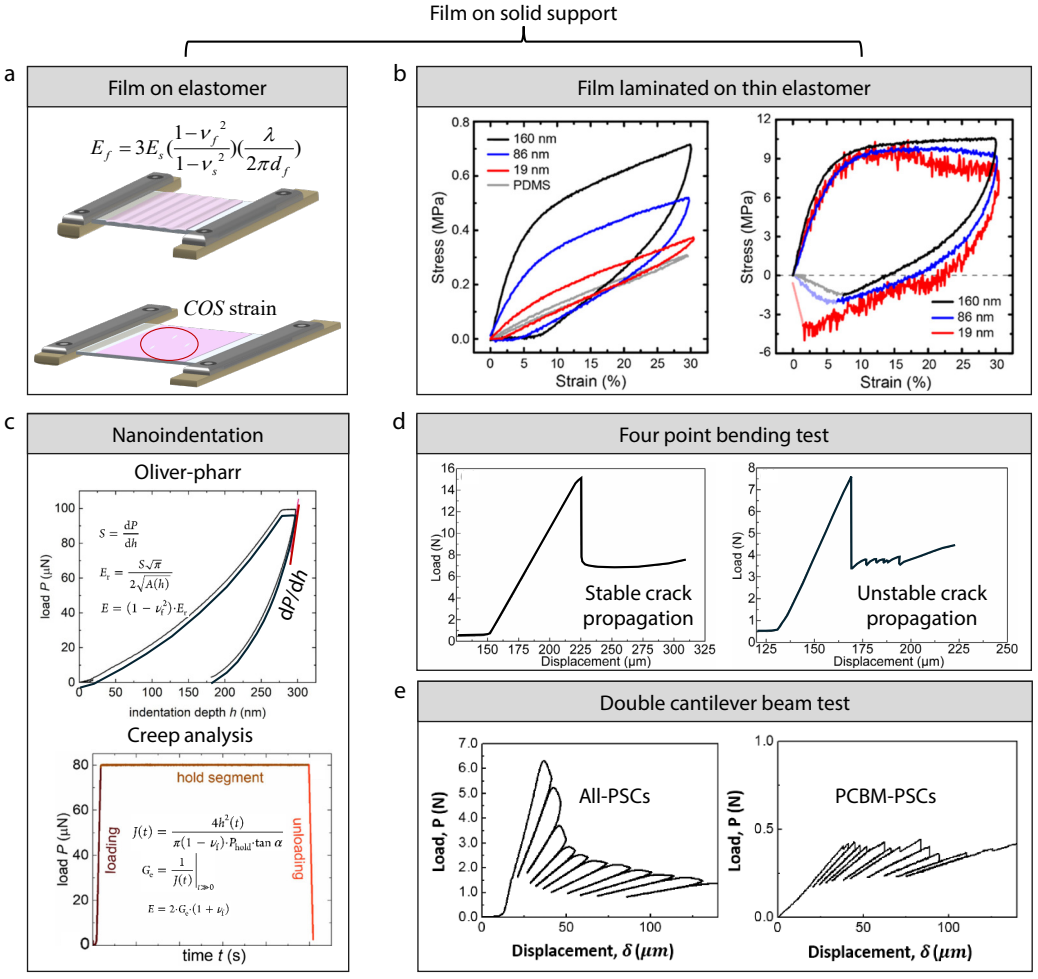

Fig. 4 Mechanical tensile testing methods for films on solid supports. (a) Schematic illustration of the FOE method. (b) Mechanical property measurements of P3HT thin films with different thicknesses performed using the FLOTE method (Reproduced with permission from Ref. [99]; Copyright (2020), American Chemical Society). (c) Two representative nanoindentation testing configurations (Reproduced with permission from Ref. [100]; Copyright (2025), American Chemical Society). (d) Force–displacement curves obtained by the FPB method, corresponding to stable and unstable crack propagation (Reproduced with permission from Ref. [42]; Copyright (2017), American Chemical Society). (e) Force–displacement curves measured by the DCB test for all-polymer solar cells and small molecule acceptor-based solar cells (Reproduced with permission from Ref. [101]; Copyright (2018), American Chemical Society).

tion. For *COS* determination, the film was transferred to an unstrained PDMS substrate and stretched using optical microscopy. The strain at which the initial cracks appeared was recorded as *COS*. Typically, slender lines perpendicular to tension appear in brittle films and dot-like shapes appear in ductile films. This parameter is vital for assessing fracture initiation in flexible devices. This technique has revolutionized the mechanical characterization of ultrathin optoelectronic polymer films by providing a simple yet powerful platform for measuring the intrinsic elastic modulus and crack-onset strain with high precision and minimal equipment requirements. Buckling-based metrology has enabled systematic studies of structure-property relationships in conjugated polymers, revealing how molecular architecture influences ductility and fracture behavior under device-relevant strains.

3.2.2 Film laminated on thin elastomer

Film lamination on a thin elastomer (FLOTE) entails laminating the polymer film onto a thin elastomer layer supported by a thicker compliant base, allowing pseudo-freestanding testing with reduced substrate effects. The process involves spin-coating the PDMS solution on a sacrificial layer to form a 2–5 μm-thick PDMS film, transferring it through water to a thicker PDMS support, and then similarly preparing and laminating the polymer film. Water immersion detached the sacrificial layer, yielding a composite specimen. O'Connor's group introduced FLOTE using the conjugated polymer P3HT as a model system, systematically examining the effects of film thickness, temperature, substrate stiffness, and loading rate on the mechanical properties (Fig. 4b).[99] Beyond standard stress-strain curves, FLOTE captures stress relaxation over broad timescales, offering insights into conjugated polymer and elastomer composites relevant to stretchable devices, and can be used to reveal how molecular packing influences viscoelastic recovery, informing strategies to mitigate fatigue in organic electronics.

3.2.3 Nanoindentation

Nanoindentation is a sophisticated depth-sensing indentation technique used to characterize the elastic and viscoelastic properties of thin polymer films. It involves the controlled penetra-

tion of a sharp indenter, which is commonly a Berkovich diamond tip, into the material surface, with simultaneous monitoring of the applied load (P) and indentation depth (h) to generate a load–displacement curve. Key parameters, such as modulus and stiffness, can be extracted using models like Oliver-Pharr (O-P),[39,102] whereas time-dependent responses enable viscoelastic analysis *via* creep or relaxation protocols (Fig. 4c). Owing to its ability to test films in situ on supporting substrates and its minimal material requirements, nanoindentation is well suited for characterizing the mechanical properties of conjugated polymer thin films. The O-P method mentioned above can analyze the initial slope of the unloading segment of $P(h)$ to extract the contact stiffness, $S = dP/dh$. Assuming that the deformation near the onset of unloading is purely elastic, the reduced modulus E_r can be obtained as follows:

$$E_r = \frac{S\sqrt{\pi}}{2\sqrt{A(h)}} \tag{4}$$

where $A(h)$ is the projected contact area determined by indenter geometry. Owing to the much higher elastic modulus of the substrate, the modulus of the film can be revised as

$$E = (1 - v_f^2) \cdot E_r \tag{5}$$

where v_f is the Poisson's ratio of the film.

Although widely used, the O-P method tends to overestimate the elastic modulus of polymer films, particularly soft or viscoelastic materials. This is because plastic deformation, pile-up around the indentation crater, and time-dependent creep increase the true contact area relative to the geometrical assumption in the O-P analysis. Consequently, the extracted modulus can deviate significantly from the intrinsic material response. Paleti *et al.* provided a rigorous reassessment of nanoindentation for conjugated polymers by directly comparing O-P analysis with creep-based nanoindentation and benchmarking against a broad suite of mechanical techniques, including tensile testing of freestanding and film on water samples, buckling analysis, AFM nanomechanics, DMA, and shear rheometry.[100] Their central finding is that creep analysis yields a far more reliable and physically meaningful modulus. During the creep analysis test, a sharp indenter was driven into the material at a controlled loading rate until a predefined load was reached. Instead of immediately unloading, which is performed in conventional Oliver-Pharr analysis, the load is held constant for a prescribed period. Throughout this hold segment, the indentation depth increased owing to viscoelastic creep, providing a direct measure of the time-dependent compliance of the material. The shear creep compliance $J(t)$ is calculated from the hold segment subsequent to rapid loading according to

$$J(t) = \frac{4h^2}{\pi(1 - v_f) \cdot P_{hold} \cdot \tan\alpha} \tag{6}$$

where the half-angle α=65.27° for the Berkovich tip and P_{hold} is the constant load applied by the indentation tip. And the long-time plateau of $J(t)$ yields the equilibrium shear modulus G_e according to

$$G_e = \frac{1}{J(t)} \,|\, t \gg 0 \tag{7}$$

assuming isotropic linear elasticity, the elastic modulus is then obtained from

$$E = 2 \cdot G_e \cdot (1 + v_f) \tag{8}$$

Using creep analysis, Paleti *et al.* determined the elastic modulus of P3HT to be 600–700 MPa, which is substantially more reliable than the 938 MPa obtained by the traditional Oliver-Pharr method, which is known to overestimate the stiffness of viscoelastic polymers. Notably, all complementary in-plane and out-of-plane techniques, including tensile testing, FOW, FOE, AFM, (dynamic mechanical thermal analysis) DMTA, and shear rheometry, yielded P3HT moduli within 300–700 MPa, with a variation of less than a factor of four. This close agreement demonstrated that P3HT behaves as an isotropic material. In contrast, the authors highlighted that highly rigid and strongly oriented polymers such as PBFDO exhibit pronounced mechanical anisotropy, requiring at least one in-plane method combined with nanoindentation to fully capture their elastic properties. This approach explicitly captures viscoelastic deformation, avoids geometric assumptions associated with unloading-based analyses, and provides a more accurate and robust determination of the elastic modulus for polymeric thin films, particularly those exhibiting significant creep or plasticity.

3.2.4 Four-point bending

The cohesive fracture energy (G_c) of conjugated polymer thin films can be measured using the four-point bending (FPB) delamination test, which is a widely adopted method for quantifying thin-film fracture toughness. The FPB specimens were prepared by constructing a multilayer sandwich structure; the polymer film was first spin-cast onto a poly(3,4-ethylenedioxythiophene):poly(styrenesulfonate)(PEDOT:PSS)-coated indium tin oxide (ITO)/glass substrate to promote cohesive rather than adhesive failure.[42,103] A thin Ca/Al bilayer was then thermally evaporated onto the film to prevent epoxy diffusion, after which a second glass slide was bonded on top using brittle epoxy adhesive and cured. The laminated structure was diced into a narrow beam, and a pre-crack notch was introduced from the glass side to localize the crack initiation. During the FPB testing, the notched specimen was loaded in a four-point geometry at a constant displacement rate, inducing controlled bending and driving interfacial crack propagation within the polymer layer (Fig. 4d). The critical load at crack initiation (P_c) was extracted from the load–displacement curve, and the cohesive fracture energy was calculated using the standard beam theory expression:

$$G_c = \frac{21P_c^2L^2}{16bh^3\bar{E}} \tag{9}$$

where L is the inner–outer pin spacing, b is the specimen width, h is the half-thickness of the glass substrate, and $\bar{E}$ is plane-strain modulus. Cohesive failure was confirmed by visual inspection and AFM imaging of the fractured surfaces, confirming that crack propagation occurred within the polymer layer rather than at the interface. This FPB approach provides a quantitative and reliable measure of the energy required to drive film fracture, enabling a direct comparison of toughness across polymer semiconductor systems.

The FPB has emerged as a highly effective and quantitative method for determining the fracture energy of photovoltaic thin-film systems.[42,103–105] O'Connor's group has employed FPB to systematically evaluate the cohesive fracture energy of

six distinct conjugated polymers.[42] Their results revealed a strong linear correlation between $(G_c/t)^{1/2}$, where t is the film thickness, and *COS*, with an impressive correlation coefficient of R=0.95 across the entire series. This universal scaling relationship allows the fracture energy of conjugated polymer films to be accurately predicted from the far more accessible *COS* measurements alone, providing an efficient and widely applicable design rule for selecting mechanically robust materials in flexible and stretchable organic electronic devices.

3.2.5 Double cantilever beam test

The double cantilever beam (DCB) test is another widely accepted technique for quantitatively measuring the cohesive fracture energy (G_c) of multilayer optoelectronic devices. A full device stack that is typically composed of glass/ITO/PEDOT:PSS/active layer/lithium fluoride (LiF) or Al is symmetrically bonded between two thick glass beams using a room-temperature-cured epoxy.[43,101,106,107] A sharp pre-crack was introduced at one edge, and the specimen was then loaded in a high-precision adhesion tester under a constant displacement rate. The specimen compliance C the fracture energy G can be calculated by:

$$C = \frac{8a^3}{Ebh^3} \tag{10}$$

$$G = \frac{P^2}{2b}\frac{\mathrm{d}C}{\mathrm{d}a} \tag{11}$$

where a is the crack length, E is the plane-strain modulus of the beam, b is the specimen width, and h is the beam thickness. In the corrected beam theory, the effective crack length is expressed as $a_{\mathrm{eff}} = a + 0.64h$, where $0.64h$ represents the end correction term. This correction accounts for the root rotation, shear deformation, and other near-tip compliance effects that are not captured by the classical Euler-Bernoulli beam theory. Incorporating this term ensures an accurate evaluation of the compliance and energy release rate, particularly for small crack lengths. The corrected calculation is as follows:

$$G = \frac{12P^2a^2}{Eb^2h^3}\left(1 + 0.64\frac{h}{a}\right)^2 \tag{12}$$

Kim *et al.* employed the DCB technique to directly compare the cohesive fracture resistance of all-polymer and fullerene-based bulk-heterojunction solar cells using the same low-bandgap donor PTB7-Th (Fig.4e).[101] At their respective optimum acceptor contents, all-polymer solar cells consist of PTB7-Th and P(NDI2HD-T) exhibited a cohesive fracture energy G = 2.45 J·m^{-2}, which is more than eight times higher than the G = 0.29 J·m^{-2} obtained for the corresponding PC71BM-based devices. This dramatic improvement stems from the intrinsically ductile polymeric acceptor, which enables extensive chain entanglement and pronounced plastic deformation during the crack propagation. The study concluded that substituting small-molecule fullerene acceptors with polymeric acceptors constitutes a simple, universal, and highly effective material strategy to dramatically enhance the mechanical robustness of high-efficiency organic solar cells, thereby enabling reliable, flexible, stretchable, and roll-to-roll processed devices.

3.3 Freestanding-film Methods

Freestanding film-based techniques represent the ultimate stage in the evolution of the static mechanical characterization of conjugated polymer thin films, as they eliminate any substrate contributions and directly yield the true intrinsic mechanical properties of the film in its device-relevant and unconfined state. By suspending ultrathin films over open microstructures or transferring them onto free-standing tensile stages, these methods provide unambiguous access to the Young's modulus, yield strength, fracture strain, toughness, and viscoelastic parameters without the complicated effects of interfacial adhesion, thermal mismatch, or substrate stiffening. Although still technically demanding, recent advances in gentle transfer protocols have transformed freestanding testing from niche capability into a practical and increasingly routine approach.

3.3.1 Camphor-assisted transfer

Camphor-assisted transfer (CAT) is a gentle method for obtaining free-standing polymer thin films. First, the polymer film was prepared on a sacrificial layer. Subsequently, a thin camphor layer was deposited on the polymer surface. After selective etching of the sacrificial layer, the camphor/polymer bilayer is released. Controlled sublimation of the camphor layer then gently lowered the intact freestanding polymer film onto the microfabricated dog-bone frames, tensile stages, or other open microstructures. Camphor-assisted transfer has been applied to graphene materials.[55,108] (Fig. 5a) Given its exceptionally gentle and damage-free nature, it is expected to see the adoption in the intrinsic mechanical characterization of conjugated polymer thin films soon.

3.3.2 Tensile tester for ultrathin freestanding films

A tensile tester for ultrathin freestanding films (TUFF) was developed by Crosby *et al.*, enabling the first direct uniaxial tensile testing of fully freestanding glassy polymer films down to 30 nm thickness.[49] After the ultrathin films are floated off onto the water surface, a custom metal frame is submerged and lifted vertically to pick up the film along three edges, overcoming capillary forces. The captured film was then cut into a dog-bone shape while still suspended across the frame. One end of the dog-bone was attached to a cantilever and the opposite end to a linear actuator, and the connecting tabs were removed, yielding a fully freestanding specimen.

The TUFF revealed a thickness-independent elastic modulus and maximum stress for 32–100 nm freestanding polystyrene films, which are in quantitative agreement with prior water-supported measurements, thereby validating the reliability of the latter in the linear-elastic regime.[45] (Fig. 5b) Critically, freestanding films exhibit substantially lower craze stability and failure strain than their water-supported counterparts. This marked reduction demonstrates that the liquid surface infiltrates nascent crazes, stabilizes fibril structures through capillary forces, and artificially enhances the large-strain ductility. Consequently, TUFF established the first true intrinsic large-deformation mechanical response of ultrathin glassy polymer films and explained the origin of the difference in mechanical response between freestanding and liquid-supported ultrathin glassy polymer films.

3.3.3 Shear motion-assisted robust transfer

Shear motion-assisted robust transfer (SMART) is a robust technique developed by Gu *et al.* for fabricating freestanding ultrathin polymer films and directly measuring their intrinsic mechanical properties.[50] The polymer solution was spin coated onto a silicon substrate with a water-soluble PSS sacrificial layer.

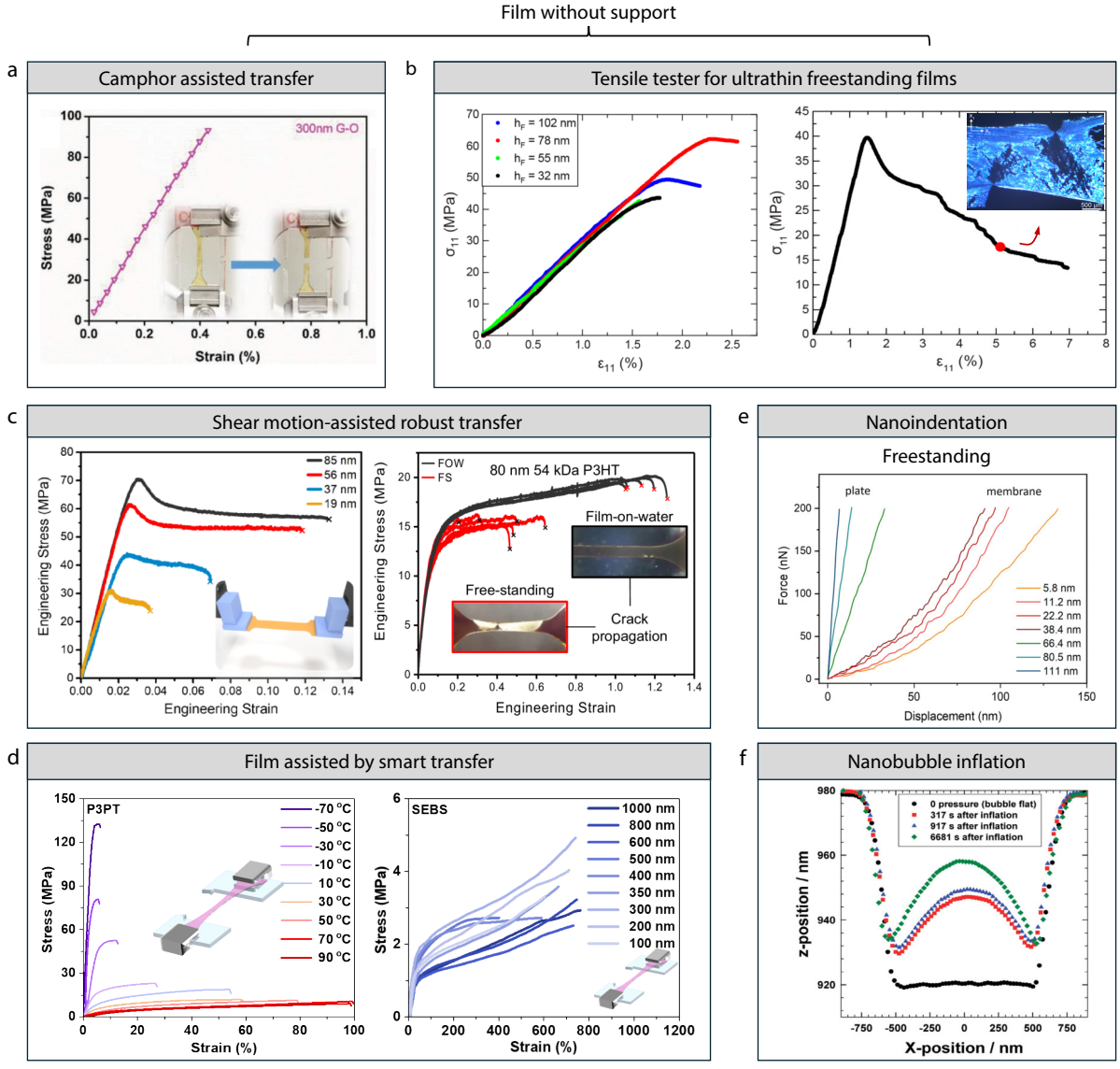

Fig. 5 Mechanical tensile testing methods for freestanding films without support. (a) Stress-strain curves of graphene oxide films measured using the CAT method (Reproduced with permission from Ref. [55]; Copyright (2018), John Wiley and Sons). (b) Stress-strain curves of PS thin films with different thicknesses and of high molecular weight PS films obtained using the TUFF method (Reproduced with permission from Ref. [49]; Copyright (2019), American Chemical Society). (c) Stress-strain curves of PS thin films with varying thicknesses measured using the SMART method, together with a comparison of stress-strain responses of P3HT films measured using the SMART and FOW methods (Reproduced with permission from Ref. [50]; Copyright (2021), Springer Nature). (d) Stress-strain curves of P3PT thin films measured at different temperatures using the FAST method, as well as stress-strain curves of SEBS thin films with different thicknesses (Reproduced with permission from Ref. [109]; Copyright (2025), American Chemical Society). Representative results obtained using the nanobubble inflation method (e) (Reproduced with permission from Ref. [48]; Copyright (2022), American Chemical Society) and nanoindentation (f) (Reproduced with permission from Ref. [110]; Copyright (2012), American Chemical Society) on freestanding thin films.

The controlled water droplets dissolved the PSS and floated the film. A motorized stage applies precise in-plane shear motion to the substrate while the film edges are gripped by clamps connected to a load cell. This shear progressively drains water from beneath the film, thereby minimizing capillary-induced damage. The fully released freestanding film was then stretched uniaxially to obtain complete stress-strain curves.

Using SMART, the authors compared the freestanding and water-supported mechanics of the PS, P3HT, and PDPP-TT films down to 19 nm (Fig. 5c). Freestanding measurements showed minor modulus differences but slightly reduced yield stress and strain at failure relative to water-supported tests, attributed to the subtle plasticizing effect of water. Thus, SMART validated the reliability of prior water-supported data while elucidating the minor yet measurable influence of water on hydrophobic polymer mechanics, providing a critical benchmark for intrinsic thin-film characterization in flexible organic electronics.

3.3.4 Freestanding film-assisted by smart transfer

Freestanding films assisted by smart transfer (FAST) is a new

method introduced by Ye's group to directly characterize the intrinsic mechanical properties of fully freestanding ultrathin conjugated polymer films. [109] The polymer solution was first spin-coated onto a glass substrate coated with a PSS sacrificial layer, forming a uniform ultrathin film, which was then laminated onto a custom poly(methyl methacrylate) (PMMA) support featuring a central I-shaped hollow by an adhesive. The composite assembly was subsequently immersed in water to dissolve the PSS layer and to detach the polymer film from the glass substrate. The ultrathin film adhering to the PMMA support was lifted vertically from the water surface to minimize capillary-induced damage. Finally, the specimen was mounted onto a tensile fixture, and the PMMA edges were melted with soldering iron to release the support, enabling uniaxial tensile testing of the fully freestanding polymer film. It should be noted that although the FAST method involves a water immersion process, its impact on the intrinsic electronic properties of the materials is generally negligible. This is primarily attributed to the universal hydrophobicity of most conjugated polymers and excellent water solubility of the PSS sacrificial layer. By applying appropriate drying treatments after the transfer process, the residual surface moisture can be effectively removed, ensuring that the thin films maintain their functional integrity following mechanical characterization.

A distinctive advantage of FAST is its seamless integration with diverse mechanical testing instruments, including universal tensile testers and dynamic mechanical analyzers. This compatibility enables the straightforward transfer of freestanding films to controlled environments, facilitating the systematic investigation of external factors such as temperature and humidity on the intrinsic mechanical behavior, which is essential for predicting the reliability of bio-integrated devices. (Fig. 5d). Therefore, this method has substantial potential for elucidating environmental influences in stretchable electronics. When applied to a diverse set of polymeric systems, including crystalline (poly(3-pentylthiophene) (P3PT)), semicrystalline (PM6), nearly amorphous (indacenodithiophene-*co*-benzothiadiazole (IDTBT)) conjugated polymers, and insulating elastomer poly(styrene-ethylene-butylene-styrene) (SEBS), FAST revealed pronounced dependencies of intrinsic modulus, yield strength, and fracture strain on film thickness, temperature, and geometry, providing essential insights for the rational design of mechanically robust stretchable polymeric semiconductors.

3.3.5 Nanoindentation on freestanding films

Nanoindentation of freestanding films creates a localized freestanding membrane environment by suspending the polymer film over microfabricated trenches in a substrate, thereby isolating intrinsic mechanics in a confined and substrate-free zone, while the surrounding areas provide structural support for handling.[48] An AFM tip applies point loading to the center of the suspended region, and the load-deflection curve is fitted to a clamped plate or membrane theory to extract the Young's modulus and stiffness. This approach effectively generates a local freestanding configuration without requiring large-area freestanding samples, minimizes handling damage, and enables high-resolution probing of nanoconfined effects (Fig. 5e).

3.3.6 Nanobubble inflation

Nanobubble Inflation is a non-contact technique for characterizing the biaxial mechanical properties of freestanding ultrathin polymer films by sealing the film over circular microcavities etched on a silicon substrate. [54,110,111] Controlled gas or liquid pressure was applied from below, to inflate the suspended membrane into a spherical cap. High-resolution optical profilometry or atomic force microscopy (AFM) monitors the central deflection height as a function of pressure. The pressure-height relationship is fitted to the classical thin-plate or membrane theory to extract the plane-strain modulus and residual stress[110] while fracture energy can be gained from a ruptured bubble(Fig. 5f).[111]

Freestanding film techniques have revolutionized the characterization of ultrathin conjugated polymer films by providing direct access to their intrinsic mechanical properties without substrate artifacts. Through innovative transfer methods such as CAT, TUFF, SMART, FAST, nanoindentation, and nanobubble inflation, researchers have uncovered thickness-dependent effects, enhanced ductility, and entropy-dominated elasticity in conjugated systems. These approaches not only resolve discrepancies between supported and unsupported measurements, but also highlight the molecular origins of size effects, such as reduced entanglement density and in-plane chain alignment, as evidenced in studies combining experimental data with molecular dynamics simulations. The maturation of these techniques promises to bridge fundamental polymer physics and device engineering, facilitating the rational design of mechanically resilient flexible electronics. By yielding benchmark intrinsic metrics, freestanding methods will enable the precise prediction of device lifetime under operational stresses, accelerating the development of next-generation optoelectronic materials with optimized performance and durability.

4 DYNAMIC MECHANICAL CHARACTERIZATION METHODS FOR CONJUGATED POLYMER THIN FILMS

The dynamic mechanical characterization of conjugated polymer thin films primarily targets key viscoelastic parameters, including the storage modulus (E'), loss modulus (E''), loss tangent (tanδ), and glass transition temperature (T_g). These metrics are essential for elucidating the time- or temperature-dependent behaviors that influence device stability and performance under operational forces. To achieve accurate measurements, particularly for ultrathin films, methods have progressively advanced from bulk samples on robust supports to more sophisticated supported and freestanding configurations. This evolution minimizes the substrate artifacts and better captures the intrinsic chain dynamics. In the following sections, we outline these methods in a logical progression, starting with early drop-casting techniques on rigid supports, transitioning to spin casting on compliant substrates, and looking toward future freestanding approaches.

4.1 Drop Casting

Drop casting serves as a foundational technique for preparing thick polymer films, which are usually more than 1 μm thick on robust supports, facilitating initial dynamic assessments using dynamic mechanical analysis instruments. These supports provide mechanical stability and compatibility with standard test-

ing setups, allowing reliable frequency or temperature sweeps. Below are the different types of support.

4.1.1 Stainless steel material pockets

Stainless steel pockets or molds act as rigid containers for the casting of bulk specimens. The process involved filling the pockets with a polymer solution, curing, and subjecting the extracted samples to DMA with controlled temperature ramps. It establishes baseline structure-property correlations, although it may overlook thin film-specific phenomena. A pioneering example of using stainless steel material pockets for the dynamic mechanical characterization of optoelectronic polymers was reported by Donald's group (Fig. 6a).[112] They prepared P3HT:PCBM blend films by drop-casting 5–10 mg of polymer solution onto cleaned stainless-steel pockets, which were subsequently folded to fully enclose the sample and dried. A dynamic mechanical thermal analysis was performed in a single cantilever bending mode. By systematically varying the PCBM content, a distinct mechanical transition of PCBM at 155 °C was identified in both neat PCBM and blends containing more than 66 wt% PCBM. The results revealed that the blends with over 70 wt% PCBM formed a single mixed phase, whereas higher PCBM loadings led to the phase separation and crystallization of PCBM. These findings highlight the critical influence of composition-dependent phase behavior on the processing conditions and morphological stability of the bulk-heterojunction active layers.

4.1.2 Polyimide support

The films are drop-casted onto flexible polyimide sheets, which offer thermal stability up to high temperatures. After curing, the assembly was clamped in a DMA fixture for oscillatory tension testing, yielding T_g and modulus data. Although straightforward, this method may overestimate the stiffness due to the substrate. Akabori *et al.* employed polyimide (PI) films as sub-

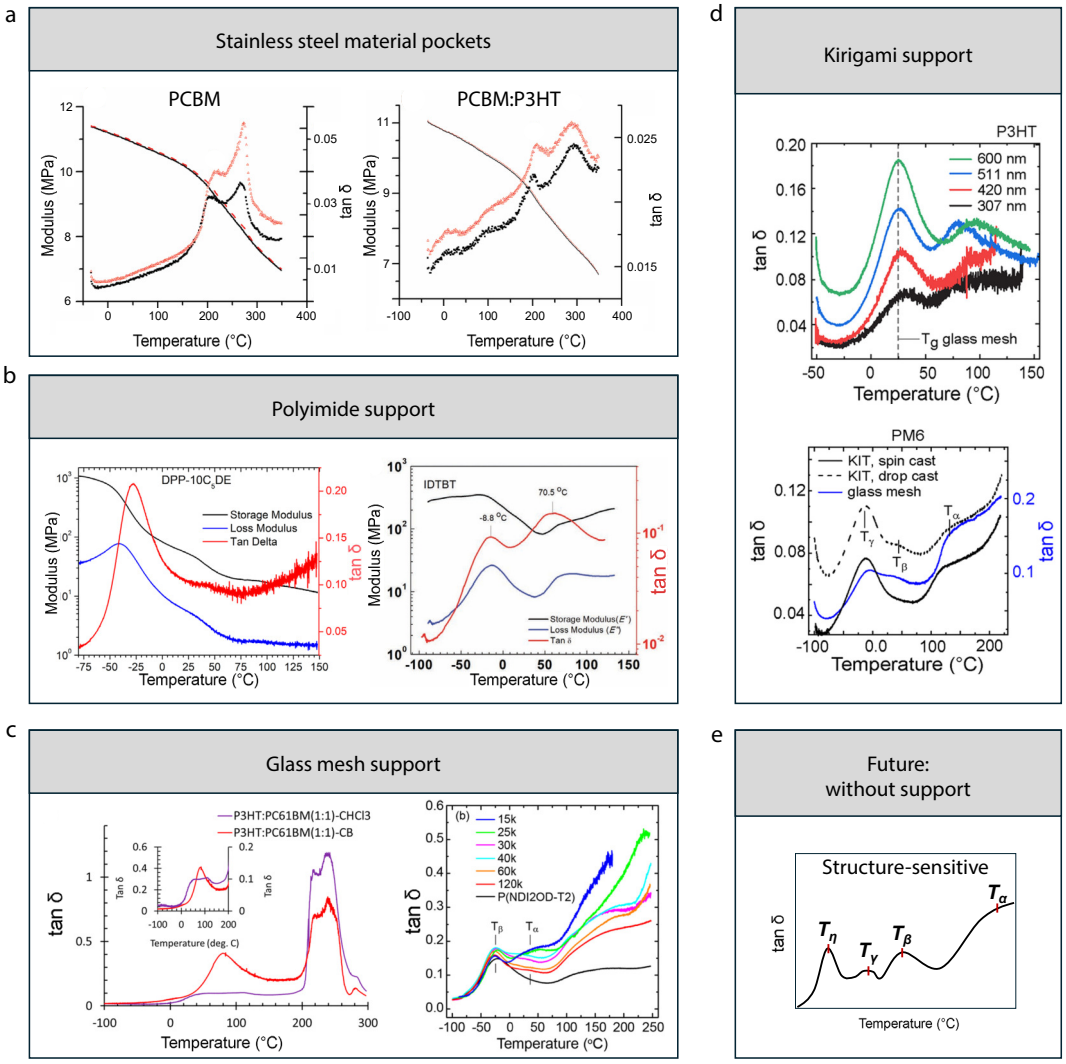

Fig. 6 Representative dynamic mechanical characterization of conjugated polymer films enabled by (a) stainless-steel material pockets (Reproduced with permission from Ref. [112]; Copyright (2011), American Chemical Society), (b) PI-supported configurations (Reproduced with permission from Refs. [113,114]; Copyright (2018), American Chemical Society and Copyright (2019), John Wiley and Sons), (c) glass mesh supports (Reproduced with permission from Refs. [61,74]; Copyright (2017), American Chemical Society and Copyright (2019), American Chemical Society), and (d) Kirigami supports (Reproduced with permission from Ref. [59]; Copyright (2021), American Chemical Society). (e) Conceptual illustration of future dynamic mechanical analysis of freestanding thin films to resolve finer structural characteristics.

https://doi.org/10.1007/s10118-026-3635-4

strates to investigate the surface effect on the molecular mobility in thin PS layers.[57] Using commercially available PI supports with a thickness of 7.5 μm which exhibited no pronounced T_g in the tested temperature range, they successfully measured PS films ranging from 30 nm to 200 nm. To further reduce substrate-induced noise, Bao's group developed an ultrathin polyimide support with a thickness of only 600 nm (Fig. 6b).[58,113,114] Using these significantly thinner compliant substrates, they performed dynamic mechanical measurements on a series of conjugated polymer thin films and obtained remarkably smooth storage or loss modulus curves with minimal background interference. Their systematic studies revealed that conjugated polymers typically exhibit two distinct glass transition regions: a low-temperature T_g between –50 and 0 °C associated with alkyl side-chain motion, and a high-temperature T_g which is usually higher than 50 °C, arising from the rigid conjugated backbone. This work clearly demonstrates that decreasing the PI substrate thickness effectively improves the signal-to-noise ratio, offering a powerful and refined platform for probing the intrinsic dynamic mechanical response of ultrathin optoelectronic polymer films.

The identification of these two regions is not only fundamental to polymer physics, but also practically significant for predicting the long-term fatigue life of flexible devices. The sub-transition associated with the side-chain motion provides a mechanism for energy dissipation through local conformational changes. At operating temperatures above the sub-, the increased molecular mobility helps to redistribute localized stresses and delays the onset of mechanical fatigue during repetitive stretching or bending cycles. The high-temperature backbone transition governs the overall morphological stability. Therefore, a well-defined separation between these transitions allows conjugated polymers to combine the structural robustness required for electronic performance with the viscoelastic resilience necessary to withstand thousands of operational cycles without catastrophic failures.

4.1.3 Glass mesh support

The use of a glass fiber mesh as a support enhances the structural integrity during testing, and this method has been widely used in glass temperature characterization (Fig. 6c).[61,62,66,74,115–128] Polymer solutions are cast onto the mesh, forming interconnected films that undergo DMA to map relaxation spectra. This approach is particularly useful for screening molecular structure effects but is less ideal for nanoscale confinement studies. Lewis *et al.* pioneered the use of a glass fiber mesh as the substrate for measuring thermal transitions in conjugated polymers by DMA, which was initially applied to characterize the thermomechanical properties of bulk heterojunction blends in polymer solar cells.[61] The glass fibers were arranged in a 45° cross-network to prevent continuous fibers from spanning the sample length and confounding the DMA signal. The samples were prepared by uniformly drop-casting polymer solutions onto the mesh, enabling reliable tensile testing. Validation across various materials revealed distinct phase separation behaviors in P3HT:$PC_{61}BM$ blends processed from chloroform versus chlorobenzene, with pronounced differences manifested at the glass transition temperature, underscoring the robustness of this method. Subsequently, leveraging this approach, the group elucidated the intrinsic correlations between the molecular structure, thermal transitions, and morphology of polymer semiconductors.[62] They observed that polymers with large alkyl side chains and flexible backbones exhibited two transitions: a sub-T_g (–80 °C to 0 °C) from side-chain motion and a primary T_g (around 100 °C) from backbone relaxation, classifying them as comprising varying amorphous and crystalline phases. In contrast, rigid backbone polymers typically show only a detectable sub-T_g, with the backbone T_g being too weak to measure because of the minimal amorphous regions, which is indicative of a hairy aggregated morphology. These insights have profound implications for flexible electronic design, inspiring numerous research groups to adopt glass-mesh DMA for groundbreaking advancements in optoelectronic polymer thin films.

4.2 Spin Casting on Robust Support

Building on drop casting, spin casting enables the formation of uniform thinner films on specialized supports, incorporating dynamic elements to probe viscoelasticity under more device-relevant conditions. These supports, which are often engineered for flexibility or pattern ability, bridge the gap between bulk and nanoscale testing. Based on the PI-supported approach, O'Connor *et al.* further advanced the technique by introducing a Kirigami-inspired support method (Fig. 6d).[59,60,129,130] They prepared 6 μm-thick polyimide substrates by spin coating and subsequently patterned them with optimized Kirigami cuts using a CO_2 laser. These precisely engineered cuts dramatically reduced the effective stiffness of the support while preserving the mechanical integrity, enabling more accurate load transfer to the polymer film of interest. Multiple conjugated polymers or blend films such as P3HT, PM6, PTB7, and PTB7-TH:IEICO-4F, primarily relevant to organic photovoltaics, were transferred onto the Kirigami-patterned PI substrates. Comparative studies have shown that the KIT method markedly outperforms conventional drop-casting and glass-mesh techniques. The proposed method has two major advantages. First, the KIT method is an evolution of the glass mesh approach, providing a compliant support that efficiently transmits oscillatory stress to the target film with minimal substrate contribution. Second, it allows the precise thermomechanical characterization of application-relevant thin films with well-defined thicknesses prepared by standard solution processing methods. Overall, the KIT strategy markedly enhances the measurement fidelity, bringing the observed relaxation temperatures closer to the intrinsic values of the ultrathin optoelectronic polymer films.

4.3 Freestanding Ultrathin-film: are True Intrinsic Properties Accessible?

The objective of dynamic mechanical characterization is to reveal the true intrinsic viscoelastic behavior of optoelectronic polymer thin films in a fully unconfined freestanding state. Although this remains a frontier for dynamic measurements, the field of static mechanical testing has already demonstrated that reliable, substrate-free characterization of ultrathin films is achievable. Multiple well-established techniques now routinely deliver accurate intrinsic modulus, strength, and toughness values without any supporting layer, proving that the gentle, high-yield transfer of nanoscale polymer membranes onto open frameworks is no longer a bottleneck. Because the same robust transfer protocols developed for static freestanding testing can be directly applied to dynamic experiments, extension to gen-

uine substrate-free dynamic mechanical analysis is both technically feasible and highly anticipated. Achieving routine free-standing dynamic measurements would, for the first time, provide true modulus and glass transition temperatures that faithfully reflect the inherent chain-segmental dynamics of ultrathin films (Fig. 6e). This is of critical importance for conjugated optoelectronic polymers, where even subtle substrate-induced perturbations in molecular packing and mobility can profoundly influence the charge transport, morphological stability, and long-term mechanical reliability in flexible and stretchable devices. With the continued refinement of non-destructive transfer techniques and sensitive non-contact detection methods, free-standing dynamic mechanical analysis is expected to be realized soon, offering the most reliable insight into the intrinsic thermomechanical response of next-generation optoelectronic polymer thin films.

5 MODULATION STRATEGIES FOR MECHANICAL PROPERTIES OF CONJUGATED POLYMER THIN FILMS

Based on the characterization techniques discussed earlier, strategies to regulate the mechanical properties of photoelectronic polymer films can be developed systematically. These approaches aim to enhance key parameters, such as the elastic modulus, fracture strain, and cohesive fracture energy, which are critical for applications in flexible and stretchable devices. Regulation can be achieved through molecular structure engineering and processing/blending strategies, leveraging insights from the confinement effects, interfacial interactions, and morphological control.

5.1 Molecular Design Strategies

The mechanical properties of conjugated polymers can be tuned by adjusting their chemical structures. In general, a rigid planar backbone yields high stiffness, whereas the introduction of flexible spacers or bulky side chains significantly softens the film (Figs. 7a–7c). For example, Paleti *et al.* showed that a polythiophene with long oligoether side chains had an elastic modulus <0.1 GPa, whereas analogous polymers without side chains, such as PEDOT:PSS, reached the GPa regime.[100] Indeed, they measured E≈47 MPa for p(g42T-T) with an oligoether side chain versus 1.34 GPa for PEDOT:PSS without side chains. The addition of flexible spacers or non-conjugated soft blocks *via* copolymerization or hydrogen-bonding motifs can also plasticize the material.[113,131–137] In addition, crosslinking represents an effective strategy for enhancing the mechanical performance of conjugated polymers (Fig. 7d). By introducing stable crosslinking points between the polymer chains, crosslinking can markedly increase the mechanical strength and elongation, while suppressing chain slippage and plastic flow.[138,139] Conversely, rigid fused-ring backbones, such as fused thiophene rings or benzodithiophene units, yield stiff and high-modulus films (Fig. 7e).[64,134] In some cases, these stiff backbones also align strongly in-plane, causing mechanical anisotropy. [100] Backbone rigidity and side-chain engineering also affect the fracture and toughness. Alkyl side chains can act as weak links that promote plastic deformation.[29,65,66] O'Connor *et al.* noted that polymers with long alkyl or oligoether chains may have better mechanical properties related to crack-onset strain to fracture energy.[42] Higher molecular weights generally increase toughness by forming more chain entanglements (Fig. 7f).[74,134] Differences in regioregularity or crystalline similarly shift the modulus: more crystalline (high-regioregularity) P3HT films were stiffer than less-crystalline ones (Fig. 7g).[134] In practice, one balances these factors; for example, copolymerizing a semiconducting segment with a rubbery block or incorporating H-bonding moieties has been shown to dramatically increase the ductility while retaining π-conjugation.

In summary, molecular design allows for wide tuning of polymer film mechanics. The introduction of flexible side chains or soft blocks yields ultralow stiffness and high extensibility, whereas all-conjugated planar backbones maximize the modulus. High-M_w, ductile polymers form extensive entanglements that increase fracture energy. Rigidity and order (high crystallinity, high T_g) increase the stiffness at the expense of stretching and can induce anisotropic elastic moduli if the chains align during film formation. Innovative molecular backbone designs have been proposed to decouple charge transport from mechanical deformation. As demonstrated by Zheng *et al*, the synergistic combination of rigid and flexible segments allows for high-mobility semiconductors that are intrinsically stretchable and resilient to cyclic strains.[141] These trends provide a molecular-level recipe for tuning the modulus, toughness, and crack strain of conjugated polymer films.

5.2 Film Casting Strategies

The processing route strongly influences the film morphology and, thus, the mechanics. Deposition methods, including spin-coating, doctor-blading, solution shearing, and interfacial spreading, can change the polymer chain orientation, packing density, and free volume. For instance, Choudhary *et al.* found that solution-shearing of poly(3-heptylthiophene) (P3HpT) films produced denser, more ordered films with higher glass transition temperatures than spin-coating.[142] Sheared films showed a much higher elastic modulus and strength than spin-coated films, while the spread films were softer but much more extensible. In their data, sheared poly(3-butylthiophene) (P3BT) also had the highest stiffness, whereas films spread on water had the highest fracture strain. This was attributed to the shear-induced chain packing, which reduced the free volume and increased the entanglements, thereby stiffening the film (Fig. 8).

The orientation of polymer chains is another key morphological factor. Films cast under shear or bar coatings often align backbones along the coating direction, yielding anisotropic elasticity.[73,142–144] Aligned films could have greatly enhanced the in-plane modulus and strength analogous to drawn fibers but may be more susceptible to cracks along the alignment direction. In contrast, isotropic films can yield similar properties in all the directions. For example, unaligned P3HT or flexible polythiophenes showed no measurable anisotropy, whereas aligned PBFDO was far stiffer along the film than along its thickness.[100]

In practice, the film morphology can be effectively tuned by controlling the solvent evaporation rate, use of processing additives, and choice of substrate.[62,75,76] Slow solvent evaporation or solvent-vapor treatments generally allow sufficient chain mobility for self-assembly, thereby enhancing crystalline order and packing density, which often leads to in-

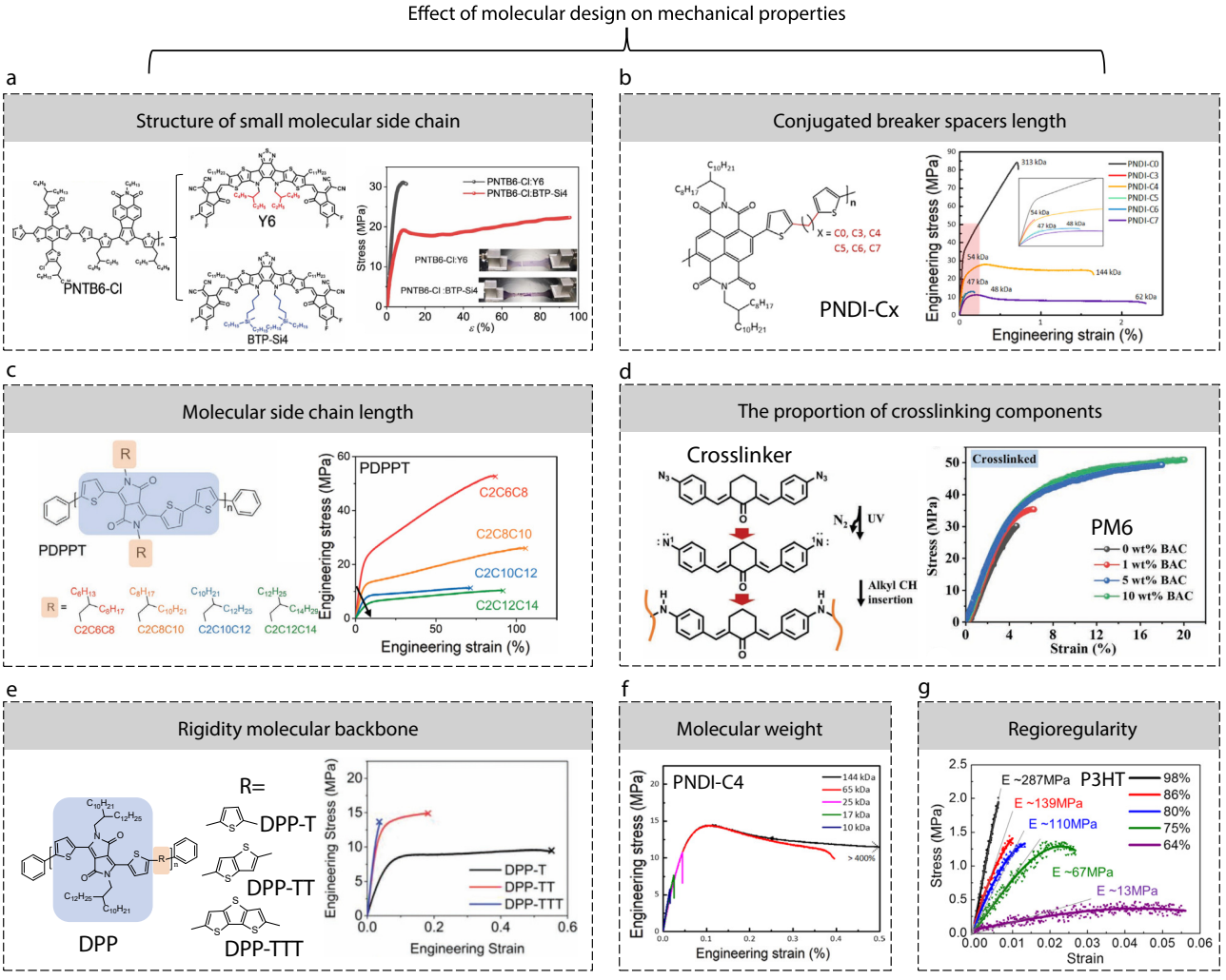

Fig. 7 Effect of molecular design on mechanical properties of optoelectronic polymer thin films. (a) Influence of side-chain molecular design (Reproduced with permission from Ref. [140]; Copyright (2018), The American Association for the Advancement of Science), (b) conjugated breaker spacer length, (c) side-chain length (Reproduced with permission from Ref. [66]; Copyright (2020), John Wiley and Sons), (d) crosslinking (proportion of crosslinker) (Reproduced with permission from Ref. [138]; Copyright (2022), John Wiley and Sons), (e) backbone rigidity (Reproduced with permission from Ref. [64]; Copyright (2019), John Wiley and Sons), (f) molecular weight (Reproduced with permission from Ref. [135]; Copyright (2020), American Chemical Society), and (g) regioregularity on mechanical properties (Reproduced with permission from Ref. [72]; Copyright (2015), American Chemical Society).

creased elastic modulus but reduced ductility due to the diminished amorphous fraction.[62,75] In contrast, rapid drying conditions or exposure to plasticizing solvent vapors can kinetically trap disordered chain conformations, resulting in more amorphous, mechanically softer films with enhanced deformability.[76] Post-deposition morphology control techniques such as thermal annealing or solvent vapor annealing further modulate this balance by promoting molecular reorganization.[67,68,73,77,78,145] Thermal annealing commonly enhances crystallization and phase separation, increasing stiffness but potentially reducing fracture strain when excessive crystallite growth or coarse phase domains are formed.[67,145] The manipulation of molecular packing and crystalline morphology is fundamental to both electronic and mechanical performance. As recently reviewed by Han *et al.*, the crystallization kinetics of donor-acceptor (D-A) conjugated polymers can be precisely controlled using solvent engineering and post-treatment protocols.[146] Such control over the degree of crystallinity and grain size is particularly crucial for thin-film mechanics, as highly crystalline domains generally enhance the elastic modulus, but may limit the overall stretchability, as discussed in previous sections. Overall, processing conditions such as the solvent, deposition method, annealing, and orientation dictate the domain structure. This, in turn, controls the distribution of strain and thus the observed modulus, anisotropy, and fracture behavior.

5.3 Additive Strategies

Mechanical performance can be dramatically altered by blending conjugated polymers with other functional additives. Blending with elastomers or rubbers is a proven method to soften composites and increase their extensibility. Recent work has shown that intimate mixing of a semiconducting polymer with a rubbery insulator such as SEBS or other specialized elastomers yields films with a low elastic modulus and very high stretch tol-

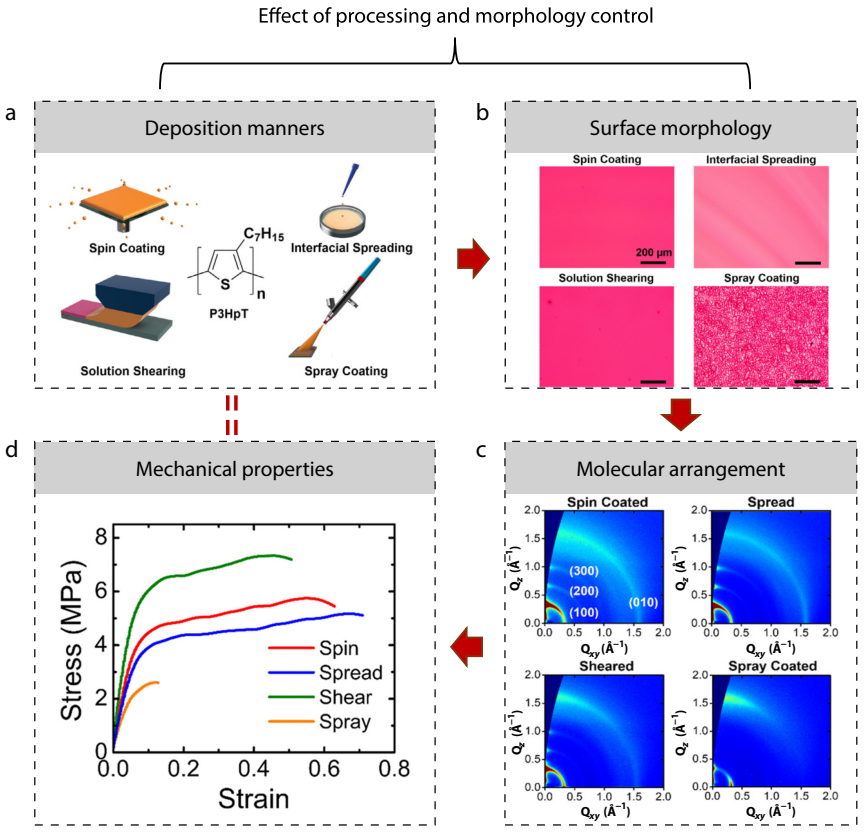

Fig. 8 Effect of processing and morphology control on mechanical properties of optoelectronic polymer thin films. (a) Mechanical behaviour under different processing conditions; (b) Surface morphology and (c) internal molecular arrangement of films processed by different methods, respectively; (d) mechanical response of films prepared under various processing conditions. (Reproduced with permission from Ref. [142]; Copyright (2021), American Chemical Society).

erance (Fig. 9a).[19,60,140,147,148–159] For example, Gao *et al.* prepared blends of high-mobility polymers consisting of PDPPTT donor and N2200 acceptor with a newly developed hydrogenated polyisoprene (H-PIP) elastomer.[147] The H-PIP blends exhibited a much lower modulus and higher crack-onset strain than the blends with conventional elastomer SEBS. In these blends, the soft elastomer matrix absorbs strain and protects the conjugated network, and the purely aliphatic, crosslink-free structure of H-PIP allowed the polymer domains to deform without generating internal stress, preserving the semiconductor pathways. In general, polymer-rubber blends behave like ductile composites: the rigid polymer fibrils bear load while the rubber dissipates strain, greatly increasing the toughness and fatigue resistance. The regulation of the elastomeric content is pivotal for balancing the competing demands of mechanical durability and electronic functions. As the weight percentage of elastomers, such as SEBS or H-PIP, increases, the composite thin films typically exhibit a progressive decrease in elastic modulus and a substantial increase in both elongation at break and crack-onset strain. This mechanical improvement stems from the ability of the elastomer to act as a stress-dissipative matrix that protects a rigid conjugated polymer network. However, excessive loading of these insulating components can lead to 'dilution' of the semiconducting phase, subsequently reducing the power conversion efficiency (PCE) or charge-carrier mobility. Recent studies have established that an optimized loading of approximately 10 wt%–20 wt% (the 'dilute-absorber' strategy) allows for a synergistic balance. In this regime, the films can maintain high-efficiency optoelectronic performance (retaining over 90% of the original PCE), while significantly extending their mechanical operational window.[147,150,152,156]

Similarly, plasticizers and small-molecule additives can lower the modulus by increasing the free volume or reducing T_g (Fig. 9b). Adding a solvent-like molecule, such as a long-chain aliphatic oil or ionic liquid, penetrates the polymer matrix and enables the sliding of chains.[149,150,160] Such plasticizers may increase the crack-onset strain at the cost of conductivity. Likewise, supramolecular dopants such as di- or tri-valent ions have been shown to increase stiffness modestly, but can also enhance interchain cohesion, depending on the interactions.[161]

Polymer-polymer blends that mix two semiconductors often yield intermediate mechanics. As noted above, blending two ductile polymers with long flexible side chains generally produces a ductile blend with toughness comparable to that of the neat polymers (Fig. 9c).[10,148,162–166] In contrast, blending with a rigid molecular filler, such as fullerene, sharply increases stiffness and reduces ductility.[101] Overall, blending offers powerful levers: elastomeric matrices and plasticizers increase ductility and fracture energy, whereas hard fillers boost the modulus but risk brittleness. By careful choice of blend partners and processing to control dispersion and interfacial adhesion, the trade-off between stiffness and toughness can be optimized. Examples such as polymer-elastomer

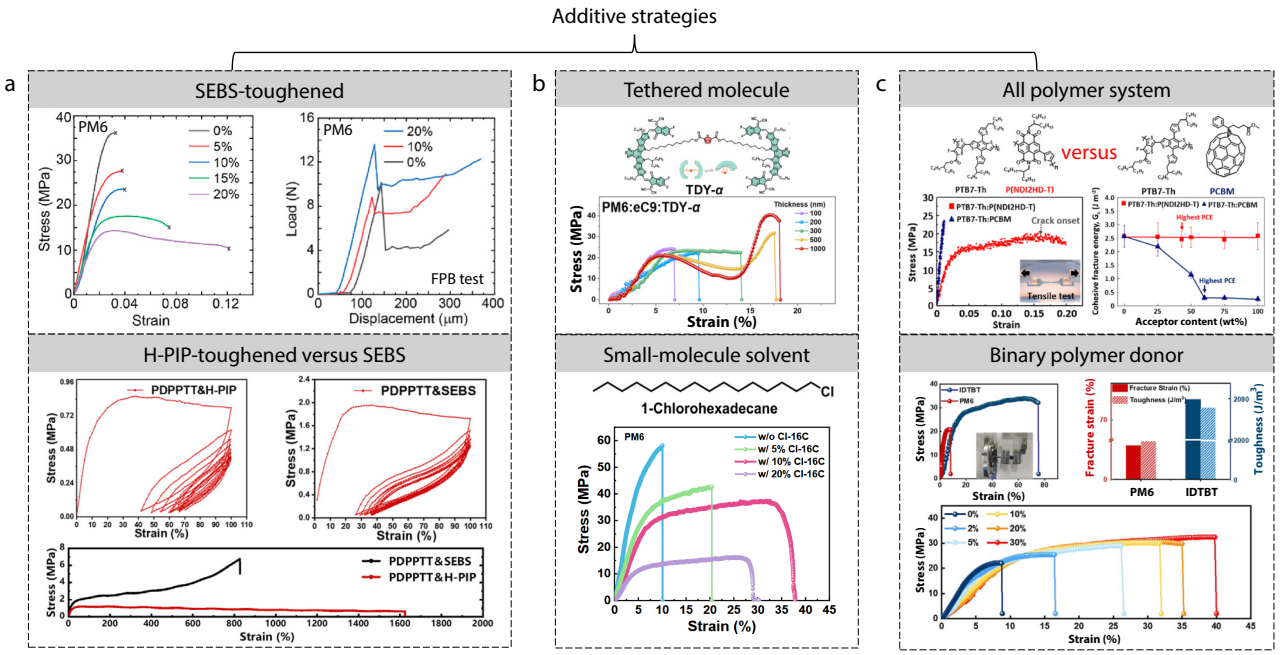

Fig. 9 Additive and blending strategies to enhance mechanical properties of optoelectronic polymer thin films. (a) Incorporation of rubbery insulators (Reproduced with permission from Refs. [60, 147]; Copyright (2023), American Chemical Society and Copyright (2025), Spring Nature). (b) Addition of small-molecule additives (Reproduced with permission from Refs. [148, 149]; Copyright (2025) The Royal Society of Chemistry). (c) Polymer blending strategies. (Reproduced with permission from Refs. [10, 101]; Copyright (2018), American Chemical Society and Copyright (2025), John Wiley and Sons).

blends, polymer-plasticizer blends, and polymer-polymer blends illustrate how additive strategies enable tailored mechanical performance in conjugated polymer films.

6 SUMMARY AND PERSPECTIVES

Mechanical characterization of conjugated polymer thin films has evolved from simple extensions of bulk methods to sophisticated techniques tailored to nanoscale confined systems. In this review, we provide a mechanical perspective on conjugated polymer thin films and summarize both static and dynamic mechanical characterization methodologies. We trace the evolution from bulk materials to substrate-supported ultrathin films and, ultimately, to freestanding ultrathin films, a progression driven by the need to accurately probe materials at length scales relevant to functional devices. The inherent challenges posed by nanoscale thickness and the often-brittle mechanical nature of conjugated polymers have spurred the development of specialized experimental platforms, such as TUFF, SMART, FAST, KIT-support, and related approaches. Collectively, these techniques form a complementary, multiscale toolbox that enables a holistic evaluation of mechanical behavior, from the elastic modulus and fracture energy to viscoelastic spectra and fatigue resistance, thereby establishing a robust experimental foundation for understanding the intrinsic mechanics of conjugated polymer ultrathin films.

Several key frontiers (Fig. 10) promise to deepen the understanding and enhance the mechanical robustness of conjugated polymer thin films for next-generation optoelectronics.

(1) Integrated *in situ* and operando characterization. Combining mechanical testing with real-time structural probes, such as grazing-incidence X-ray scattering (GIWAXS/GISAXS),[15,151] Raman spectroscopy, or AFM, will enable a direct correlation between the imposed deformation and the dynamic evolution of chain packing, crystalline domain orientation, and crack initiation. This bridges the gap between the macroscopic mechanical response and the nanoscale structural changes under operational strain.

(2) High-throughput and combinatorial screening. Accelerating the discovery of mechanically robust conjugated polymer systems requires the development of platforms that can rapidly screen polymer libraries, blends, and processing conditions. Miniaturized tensile stages, automated buckling metrology, and parallelized nanoindentation, coupled with machine-learning-assisted data analysis, could significantly shorten the design-test-optimize cycle for stretchable polymer semiconductors.

(3) Fatigue and long-term reliability tests. Most current studies have focused on a single-cycle or monotonic loading. For practical wearable and implantable electronics, understanding the fatigue life, crack propagation under cyclic strain, and environmental aging (*e.g.*, humidity, temperature cycling, and ultraviolet (UV) exposure) is essential. Standardized protocols for assessing the mechanical endurance under realistic operating conditions must be established.

(4) Multiphysics modeling across scales. Computational frameworks that connect atomistic molecular dynamics, coarse-grained polymer models, and continuum mechanical simulations can predict not only elastic and plastic responses, but also how mechanical deformation alters electronic properties (*e.g.*, mobility and recombination) through conformational changes, trap formation, or interfacial decohesion.

(5) Standardization of measurement protocols. As the field matures, community-wide agreement on testing parameters,

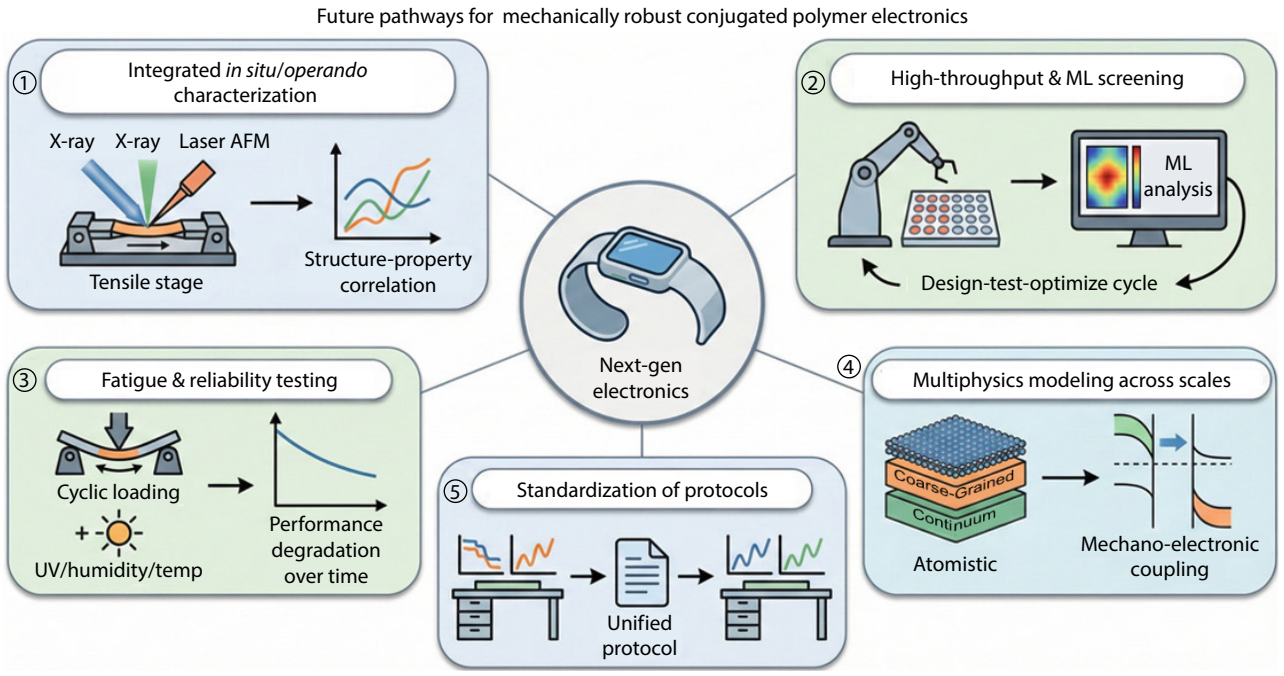

Fig. 10 Future perspective on mechanically robust conjugated polymer electronics. The schematic highlights five critical, synergistic research areas requisite for realizing next-generation flexible electronics: (1) advanced *in situ* and operando characterization, (2) machine-learning-assisted high-throughput screening, (3) rigorous fatigue and environmental reliability testing, (4) multiscale computational modeling, and (5) standardization of testing protocols. Collectively, these strategies form the core pathway from fundamental understanding to technology translation.

e.g. as strain rates, sample geometries, environmental control, and data analysis methods, will be crucial for enabling reproducible and comparable datasets across laboratories and accelerating technology transfer.

By embracing these interdisciplinary opportunities, the field can progress from empirical testing/tuning to predictive design, ultimately enabling the creation of conjugated polymer thin films that are not only electronically efficient, but also mechanically dependable in real-world flexible and stretchable applications.

Although advances in characterization are rapidly expanding and can be measured and reliably compared across studies, a parallel challenge is to translate these measurements into actionable design rules. In practice, mechanical robustness is not an intrinsic "single-parameter" property; rather, it emerges from the hierarchy of structural determinants and processing-dependent morphologies. Therefore, establishing clear structure-process-mechanics relationships is essential for interpreting the rich datasets enabled by modern platforms and rationally tuning films toward device-relevant mechanical targets.

The mechanical behavior of conjugated polymer thin films is governed by multiple strongly coupled factors spanning the molecular to device length scales. At the molecular level, backbone rigidity, side-chain architecture, molecular weight, and its distribution determine the fundamental balance between stiffness, ductility, and time-dependent relaxation. At the mesoscale, crystallinity, chain orientation, and phase morphology (including the nature of amorphous/crystalline interphases) modulate the load transfer, plasticity, and viscoelastic dissipation. At the film and interface levels, the processing routes (*e.g.*, coating/printing methods), post-treatment (thermal or solvent annealing), residual stress, and interfacial interactions with substrates further define the effective mechanical response and failure pathways. Importantly, formulation strategies, such as blending with elastomeric or ductile components, incorporating small-molecule additives, or introducing crosslinkable motifs, can reconfigure the percolation of rigid domains, tune segmental mobility, and redistribute stress concentrations, thereby altering both toughness and fatigue resistance. As these parameters are interdependent, selecting and combining appropriate regulation strategies is critical for optimizing conjugated polymer thin films for mechanically reliable optoelectronic applications.

Looking ahead, the effective characterization and regulation of mechanical properties should adopt an application-oriented, iterative framework that closes the loop between device requirements, material design, and quantitative testing (Fig. 11). The first step is to define the mechanical envelope required by the target device and its operating conditions (*e.g.*, allowable strain, bending radius, cyclic durability, and thermal/humidity exposure). Guided by these constraints, polymer molecular design, processing optimization, and formulation engineering can be deployed in a purpose-driven manner to shift the film into the desired performance window (*e.g.*, soft-yet-resilient for stretchable electronics or stiff-yet-crack-resistant for robust coatings). Comprehensive mechanical characterization, which is performed not only on isolated films but also on device-relevant stacks and under realistic loading modes and environments, should then be used to identify the dominant deformation and failure mechanisms. The resulting insights can be used to refine molecular

https://doi.org/10.1007/s10118-026-3635-4

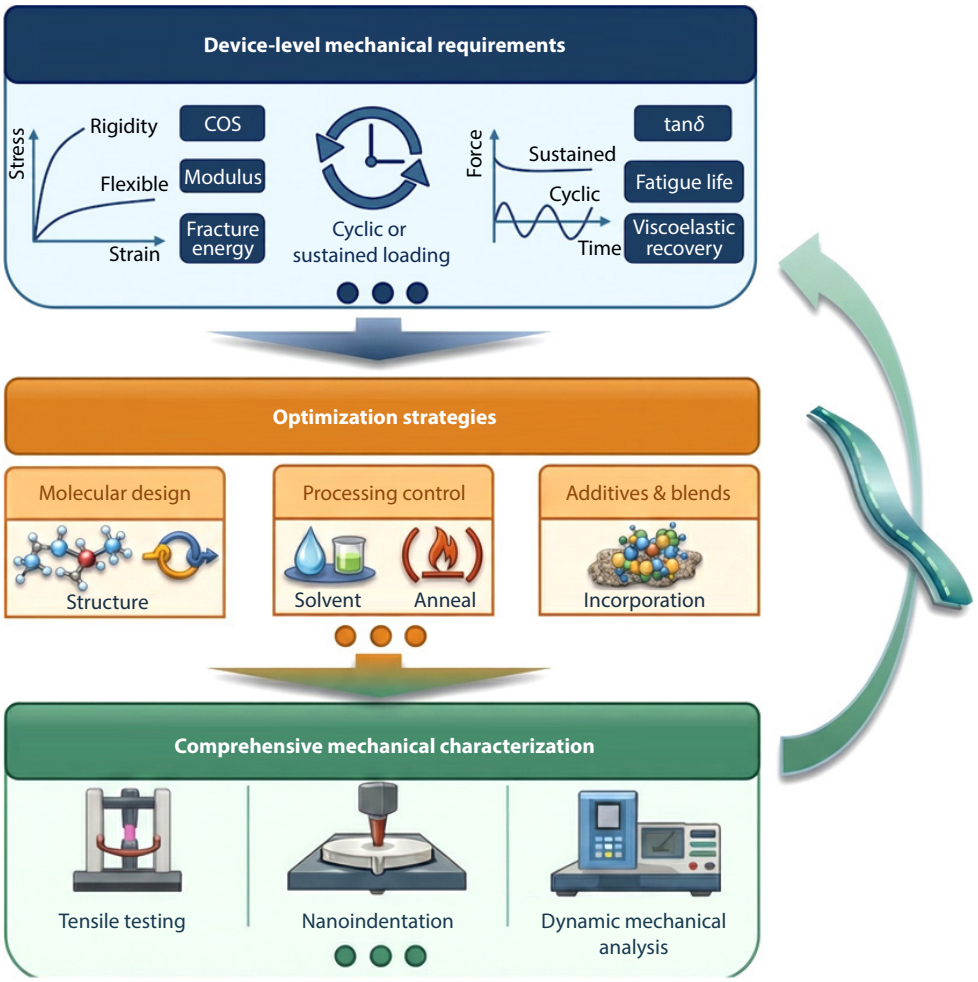

Fig. 11 An integrated framework for the design and optimization of mechanically robust conjugated polymer thin films for stretchable organic optoelectronics. The framework is a feedback-driven cycle guided by application-specific mechanical demands.

structures, morphology control, and interfacial engineering, iterating until both mechanical reliability and optoelectronic functionality are simultaneously satisfied. Overall, this review outlines a coherent pathway that connects characterization methodologies to structure–property relationships and application needs, providing a practical reference for the rational mechanical design and regulation of optoelectronic polymer thin films.

Furthermore, as the field moves toward seamless bio-integrated electronics, achieving mechanical compatibility with biological tissues has become a critical requirement. To ensure long-term biocompatibility and stable signal acquisition, conjugated polymer thin films must be designed to match the low modulus and high compliance of soft tissues that often exhibit elastic moduli ranging from kilopascals to megapascals. Future innovations in molecular engineering and composite formulations will play a pivotal role in bridging the mechanical gap between rigid electronic materials and soft biological systems.

BIOGRAPHY

2026 Rising Scholar: Long Ye has been a professor at the School of Materials Science and Engineering, Tianjin University since October 2019. He received his PhD degree from the Institute of Chemistry, Chinese Academy of Sciences in 2015 (Advisor: Prof. Jianhui Hou). From 2015 to 2019, he was a postdoctoral researcher (Advisor: Prof. Harald Ade) and later promoted to research assistant professor at the Department of Physics, North Carolina State University. His current interests include flexible/stretchable organic optoelectronic devices and related materials physics (*e.g.*, aggreate structure, thermodynamics, mechanics).

Conflict of Interests

The authors declare no interest conflict.

ACKNOWLEDGMENTS

This work was financially supported by the Science Fund for Distinguished Young Scholars of Tianjin Municipality (No. 23JCJQJC00240), the National Natural Science Foundation of China (No. 52121002), and Opening Project of Hubei Longzhong Laboratory (No. 2022KF-01). We also sincerely

appreciate the Fundamental Research Funds for Central Universities for their continuous support.

REFERENCES

1 Zhong, D.; Wu, C.; Jiang, Y.; Yuan, Y.; Kim, M. G.; Nishio, Y.; Shih, C. C.; Wang, W.; Lai, J. C.; Ji, X.; Gao, T. Z.; Wang, Y. X.; Xu, C.; Zheng, Y.; Yu, Z.; Gong, H.; Matsuhisa, N.; Zhao, C.; Lei, Y.; Liu, D.; Zhang, S.; Ochiai, Y.; Liu, S.; Wei, S.; Tok, J. B. H.; Bao, Z. High-speed and large-scale intrinsically stretchable integrated circuits. *Nature* **2024**, *627*, 313–320.

2 Zuo, J.; Han, D.; Yao, H.; Kuvondikov, V.; Ye, L. Stretching the future: Strategies and emerging trends in stretchable organic photovoltaic materials. *Energy Environ. Sci.* **2025**, *18*, 6344–6365.

3 Li, S.; Liu, J.; Kuvondikov, V.; Yan, J.; Ye, L. Organic photovoltaics generate more power under stretching. *Matter* **2025**, *8*, 102062.

4 Wijaya, T. J.; Xiong, S.; Sasaki, K.; Kato, Y.; Mori, K.; Koizumi, M.; Lee, S.; Kobayashi, M.; Zhou, Y.; Fukuda, K.; Yokota, T.; Someya, T. A highly stable organic–inorganic hybrid electron transport layer for ultraflexible organic photodiodes. *Adv. Mater.* **2025**, *37*, 2501951.

5 Lee, J. W.; Oh, E. S.; Lee, S.; Phan, T. N. L.; Kim, T. S.; Lee, J. Y.; Reynolds, J. R.; Kim, B. J. Strain-induced power output enhancement in intrinsically stretchable organic solar cells. *Joule* **2025**, *9*, 101792.

6 Shi, Y.; Zhang, B.; Zhao, J.; Qin, J.; Bai, K.; Yu, J.; Zhang, X. A deformation mismatch strategy enables over 120% stretchability of encapsulated serpentine silicon strips for stretchable electronics. *FlexMat* **2024**, *1*, 150–159.

7 Lu, X.; Xie, C.; Liu, Y.; Zheng, H.; Feng, K.; Xiong, Z.; Wei, W.; Zhou, Y. Increase in the efficiency and stability of large-area flexible organic photovoltaic modules *via* improved electrical contact. *Nat. Energy* **2024**, *9*, 793–802.

8 Oh, J. Y.; Rondeau-Gagné, S.; Chiu, Y. C.; Chortos, A.; Lissel, F.; Wang, G. J. N.; Schroeder, B. C.; Kurosawa, T.; Lopez, J.; Katsumata, T.; Xu, J.; Zhu, C.; Gu, X.; Bae, W. G.; Kim, Y.; Jin, L.; Chung, J. W.; Tok, J. B. H.; Bao, Z. Intrinsically stretchable and healable semiconducting polymer for organic transistors. *Nature* **2016**, *539*, 411–415.

9 Zhang, Z.; Li, P.; Xiong, M.; Zhang, L.; Chen, J.; Lei, X.; Pan, X.; Wang, X.; Deng, X.-Y.; Shen, W.; Mei, Z.; Liu, K.-K.; Liu, G.; Huang, Z.; Lv, S.; Shao, Y.; Lei, T. Continuous production of ultratough semiconducting polymer fibers with high electronic performance. *Sci. Adv.* **2024**, *10*, eadk0647.

10 Ke, H.; Xie, H.; Pei, L.; Gao, M.; Li, S.; Sheng, D.; Urazkulova, D.; Kuvondikov, V.; Nematov, S.; Li, X.; Ye, L. Mechanically stable and intrinsically stretchy organic photovoltaics *via* constructing stress-dissipative networks. *Chin. J. Chem* **2025**, *43*, 2909–2916.

11 Chen, H.; Huang, Y.; Zhang, R.; Mou, H.; Ding, J.; Zhou, J.; Wang, Z.; Li, H.; Chen, W.; Zhu, J.; Cheng, Q.; Gu, H.; Wu, X.; Zhang, T.; Wang, Y.; Zhu, H.; Xie, Z.; Gao, F.; Li, Y.; Li, Y. Organic solar cells with 20.82% efficiency and high tolerance of active layer

Graphical Abstract

Advancing the Thin-film Mechanics of Conjugated Polymers: Characterization, Modulation, and Innovation

Jin-Tao Feng and Long Ye

Tianjin University

This review establishes a tripartite framework for conjugated polymer mechanics, spanning multiscale characterization, molecular and morphological engineering, and architectural innovation toward tailored functionality and bio-integrated electronics.

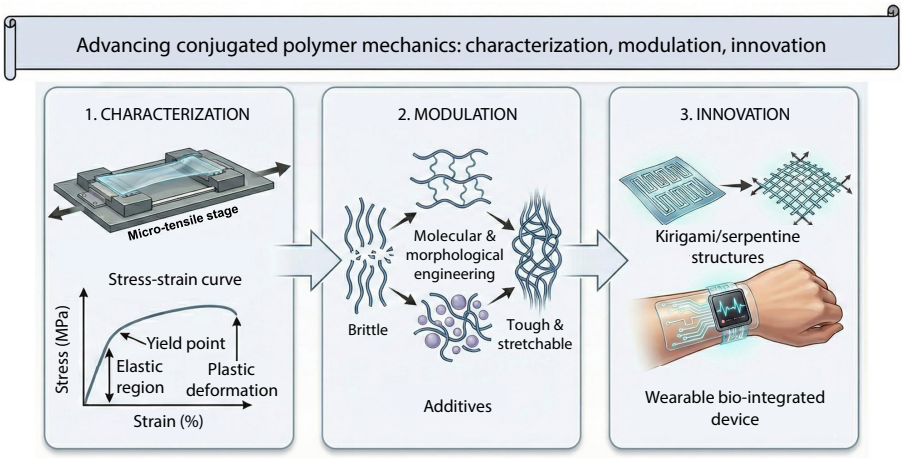

Chinese J. Polym. Sci. 2026, 44, 2086–2111 *https://doi.org/10.1007/s10118-026-3635-4*

thickness through crystallization sequence manipulation. *Nat. Mater.* **2025**, *24*, 444–453.
12 Song, W.; Ye, Q.; Chen, Z.; Ge, J.; Xie, L.; Ge, Z. Advances in stretchable organic photovoltaics: Flexible transparent electrodes and deformable active layer design. *Adv. Mater.* **2024**, *36*, 2311170.
13 Brabec, C. J.; Distler, A.; Du, X.; Egelhaaf, H. J.; Hauch, J.; Heumueller, T.; Li, N. Material strategies to accelerate OPV technology toward a GW technology. *Adv. Energy Mater.* **2020**, *10*, 2001864.
14 Bae, Y.; Kim, D.; Li, S.; Choi, Y.; Son, S. Y.; Park, T.; Ye, L. Stability of intrinsically stretchable polymer photovoltaics: Fundamentals, achievements, and perspectives. *Prog. Polym. Sci.* **2024**, *159*, 101899.
15 Chen, Y.; Li, S.; Shen, Z.; Sun, C.; Feng, J.; Ye, L. In-situ temperature-controllable grazing incidence X-ray scattering of semiconducting polymer thin films under stretching. *Sci. China Mater.* **2024**, *67*, 3917–3924.
16 Lin, C.; Chen, Z.; Peng, R.; Song, W.; Gao, J.; Yu, X.; Feng, T.; Bai, Y.; Ge, Z. Flexible spacer-block multi-component copolymerized donors enable resilient organic solar cells with over 40% crack-onset strain. *Energy Environ. Sci.* **2024**, *17*, 9359–9374.
17 Li, H.; Zeng, S.; Zhao, H.; Liu, Q.; Xue, T.; Liu, S.; Li, H.; Hu, L.; Zhou, E.; Khumalo, M.; Hu, X.; Chen, Y. Molecularly interlocked interfaces enable record-efficiency stretchable organic photovoltaics. *Adv. Mater.* **2025**, *37*, 2507761.
18 Yang, S.; Chen, X.; Pan, Y.; Fang, J.; Han, Y.; Wang, Z.; Qian, F.; Qi, W.; Shui, K.; Zhang, Q.; Guo, F.; Sun, Y.; Ma, C.-Q.; Luo, Q. High cell to module efficiency remaining ratio of ≈90% for the 100 cm^2 fully roll-to-roll gravure printed flexible organic solar cells from non-halogenated solvent. *Adv. Mater.* **2025**, *37*, 2500115.
19 Tang, W.; Ding, Z.; Su, Y.; Weng, Q.; Zhang, Y.; Li, R.; Huang, W.; Wang, Z.; Wu, Y.; Han, Y.; Zhao, K.; Yang, Z.; Wang, X.; Liu, S. Sequentially deposited elastomer-based ternary active layer for high-performance stretchable organic solar cells. *Adv. Funct. Mater.* **2024**, *34*, 2312289.
20 Xiao, Z.; Liu, J.; Chen, X.; Suo, Z.; Cao, X.; Xu, N.; Yao, Z.; Li, C.; Wan, X.; Chen, Y. Ultra-flexible organic solar cells based on eco-friendly cellulose substrate with efficiency approaching 19%. *J. Mater. Chem. A* **2025**, *13*, 2301–2308.
21 Jiang, Y.; Sun, S.; Xu, R.; Liu, F.; Miao, X.; Ran, G.; Liu, K.; Yi, Y.; Zhang, W.; Zhu, X. Non-fullerene acceptor with asymmetric structure and phenyl-substituted alkyl side chain for 20.2% efficiency organic solar cells. *Nat. Energy* **2024**, *9*, 975–986.
22 Zhang, K.; Gao, M.; Wu, J.; Sun, C.; Zhao, W.; Urazkulova, D.; Kuvondikov, V.; Nematov, S.; Ye, L. Cost-effective poly(3-alkylthiophene)-based organic photovoltaics: Advancing solar energy conversion and photodetection technologies. *Mater. Horiz.* **2025**, *12*, 8832–8861.
23 Zhang, K.; Wu, J.; Sun, C.; Chung, D. S.; Geng, Y.; Ye, L. The rising promise of organic photodetectors in emerging technologies. *Nat. Rev. Mater.* **2025**, *10*, 487–489.
24 Du, B.; Xiong, S.; Sun, L.; Tagawa, Y.; Inoue, D.; Hashizume, D.; Wang, W.; Guo, R.; Yokota, T.; Wang, S.; Ishida, Y.; Lee, S.; Fukuda, K.; Someya, T. A water-resistant, ultrathin, conformable organic photodetector for vital sign monitoring. *Sci. Adv.* **2024**, *10*, eadp2679.
25 He, X.; Li, Y.; Yu, H.; Zhou, G.; Ke, L.; Yip, H.-L.; Zhao, N. A microsized optical spectrometer based on an organic photodetector with an electrically tunable spectral response. *Nat. Electron.* **2024**, *7*, 694–704.
26 Woo, J. Y.; Park, M. H.; Jeong, S. H.; Kim, Y. H.; Kim, B.; Lee, T. W.; Han, T. H. Advances in solution-processed OLEDs and their prospects for use in displays. *Adv. Mater.* **2023**, *35*, 2207454.
27 Kim, D.; Park, H. J.; Jung, S. H.; Pyo, W. J.; Hassan, S. Z.; Sim, H. R.; Lee, J. H.; Jee, D. W.; Chung, D. S. Visible-light communication with lighting: RGB wavelength division multiplexing oleds/opds platform. *Adv. Mater.* **2024**, *36*, 2309416.
28 Ma, J.; Xu, M.; Zhuo, Z.; Wang, K.; Li, Q.; Li, H.; Feng, Q.; Chen, W.; Yu, N.; Li, M.; Xie, L.; Lin, J. Plasticizer design principle of "like dissolves like": Semiconductor fluid plasticized stretchable fully π-conjugated polymers films for uniform large-area and flexible deep-blue polymer light-emitting diodes. *Adv. Mater.* **2024**, *36*, 2411449.
29 Chen, W.; Yu, N.; Gong, H.; Li, M.; Xu, W.; Zhuo, Z.; Sun, Z.; Ni, M.; Huang, W.; Yang, J.; Lin, Y.; Wang, L.; Li, H.; Liang, X.; Sun, N.; Sun, L.; Bai, L.; Han, Y.; Tao, Y.; Xu, M.; Yin, C.; An, X.; Lin, J.; Huang, W. Elastic–plastic fully π-conjugated polymer with excellent energy dissipation capacity for ultra-deep-blue flexible polymer light-emitting diodes with CIEy = 0.04. *Adv. Mater.* **2024**, *36*, 2402708.
30 Zhang, Z.; Wang, W.; Jiang, Y.; Wang, Y.-X.; Wu, Y.; Lai, J.-C.; Niu, S.; Xu, C.; Shih, C.-C.; Wang, C.; Yan, H.; Galuska, L.; Prine, N.; Wu, H.-C.; Zhong, D.; Chen, G.; Matsuhisa, N.; Zheng, Y.; Yu, Z.; Wang, Y.; Dauskardt, R.; Gu, X.; Tok, J. B. H.; Bao, Z. High-brightness all-polymer stretchable LED with charge-trapping dilution. *Nature* **2022**, *603*, 624–630.
31 Jeong, M. W.; Ma, J. H.; Shin, J. S.; Kim, J. S.; Ma, G.; Nam, T. U.; Gu, X.; Kang, S. J.; Oh, J. Y. Intrinsically stretchable three primary light-emitting films enabled by elastomer blend for polymer light-emitting diodes. *Sci. Adv.* **2023**, *9*, eadh1504.
32 Wang, J.; Ren, Z.; Yan, T.; Jia, R.; Cheng, Y.; Zhang, X.; Jie, J. Floating epitaxy and stitching growth of bilayer organic semiconductor single crystals on polymer dielectric toward high-performance and ultra-flexible transistors. *Adv. Mater.* **2026**, *38*, e15477.
33 Sun, J.; Zhao, G.; Zhang, M.; Zhao, X.; Tong, Y.; Tang, Q.; Liu, Y. Intrinsically stretchable organic field-effect transistors: Progress and challenges. *J. Mater. Chem. C* **2024**, *12*, 6011–6026.
34 Zheng, X.; Zhao, Y.; Li, X.; Zhang, X.; Yang, H.; Ye, X.; Yang, H.; Hu, W. Ionic additive enhanced stability of stretchable polymer composites for gas sensing based on stretchable OFET. *Chem. Eng. J.* **2025**, *523*, 168342.
35 Ding, Y.; Xu, X.; Wu, Y.; Zhang, H.; Shao, L.; Wang, Z.; Zhang, H.; Zhao, Y.; Liu, Y. Reconfigurable dual-gate ferroelectric field-effect transistors based on semiconducting polymer for logic operations and synaptic applications. *SmartMat* **2025**, *6*, e70003.
36 Zang, Y.; Huang, D.; Di, C.-a.; Zhu, D. Device engineered organic transistors for flexible sensing applications. *Adv. Mater.* **2016**, *28*, 4549–4555.
37 Cao, Y.; Smith, P.; Heeger, A. J. Mechanical and electrical properties of polyacetylene films oriented by tensile drawing. *Polymer* **1991**, *32*, 1210–1218.
38 Baklar, M. A.; Koch, F.; Kumar, A.; Domingo, E. B.; Campoy-Quiles, M.; Feldman, K.; Yu, L.; Wobkenberg, P.; Ball, J.; Wilson, R. M.; McCulloch, I.; Kreouzis, T.; Heeney, M.; Anthopoulos, T.; Smith, P.; Stingelin, N. Solid-state processing of organic semiconductors. *Adv. Mater.* **2010**, *22*, 3942–3947.
39 Strojny, A.; Xinyun, X.; Tsou, A.; Gerberich, W. W. Techniques and considerations for nanoindentation measurements of polymer thin film constitutive properties. *J. Adhes. Sci. Technol.* **1998**, *12*, 1299–1321.
40 Stafford, C. M.; Harrison, C.; Beers, K. L.; Karim, A.; Amis, E. J.; VanLandingham, M. R.; Kim, H. C.; Volksen, W.; Miller, R. D.; Simonyi, E. E. A buckling-based metrology for measuring the elastic moduli of polymeric thin films. *Nat. Mater.* **2004**, *3*, 545–550.

https://doi.org/10.1007/s10118-026-3635-4

41 Stafford, C. M.; Guo, S.; Harrison, C.; Chiang, M. Y. M. Combinatorial and high-throughput measurements of the modulus of thin polymer films. *Rev. Sci. Instrum.* **2005**, *76*, 062207.

42 Balar, N.; O'Connor, B. T. Correlating crack onset strain and cohesive fracture energy in polymer semiconductor films. *Macromolecules* **2017**, *50*, 8611–8618.

43 Lee, J.; Lee, J. W.; Song, H.; Song, M.; Park, J.; Kim, G. U.; Jeong, D.; Kim, T. S.; Kim, B. J. Interdiffused thermoplastic urethane-PEDOT:PSS bilayers with superior adhesion properties for high-performance and intrinsically-stretchable organic solar cells. *J. Mater. Chem. A* **2023**, *11*, 12846–12855.

44 Kim, J. H.; Nizami, A.; Hwangbo, Y.; Jang, B.; Lee, H. J.; Woo, C. S.; Hyun, S.; Kim, T. S. Tensile testing of ultra-thin films on water surface. *Nat. Commun.* **2013**, *4*, 2520.

45 Liu, Y.; Chen, Y. C.; Hutchens, S.; Lawrence, J.; Emrick, T.; Crosby, A. J. Directly measuring the complete stress–strain response of ultrathin polymer films. *Macromolecules* **2015**, *48*, 6534–6540.

46 Lee, T. I.; Kim, J. H.; Oh, E. S.; Kim, T. S. Direct tensile testing of free-standing ultrathin polymer films on liquid surface at high temperature. *Small Methods* **2025**, *9*, 2401291.

47 Zhang, S.; Koizumi, M.; Cao, Z.; Mao, K. S.; Qian, Z.; Galuska, L. A.; Jin, L.; Gu, X. Directly probing the fracture behavior of ultrathin polymeric films. *ACS Polym. Au* **2021**, *1*, 16–29.

48 Wang, G.; Najafi, F.; Ho, K.; Hamidinejad, M.; Cui, T.; Walker, G. C.; Singh, C. V.; Filleter, T. Mechanical size effect of freestanding nanoconfined polymer films. *Macromolecules* **2022**, *55*, 1248–1259.

49 Bay, R. K.; Crosby, A. J. Uniaxial extension of ultrathin freestanding polymer films. *ACS Macro Lett.* **2019**, *8*, 1080–1085.

50 Galuska, L. A.; Muckley, E. S.; Cao, Z.; Ehlenberg, D. F.; Qian, Z.; Zhang, S.; Rondeau-Gagné, S.; Phan, M. D.; Ankner, J. F.; Ivanov, I. N.; Gu, X. SMART transfer method to directly compare the mechanical response of water-supported and free-standing ultrathin polymeric films. *Nat. Commun.* **2021**, *12*, 2347.

51 Zhang, H.; Fujiki, K.; Ido, K.; Kusayanagi, N.; Sakagami, D.; Li, J.; Okamura, Y. Tensile testing of freestanding polymer thin films with non-standard geometries. *Polym. Test.* **2020**, *91*, 106825.

52 Bae, J. S.; Oh, C. S.; Nam, J. E.; Lee, J. K.; Lee, H. J. A tensile test technique for the freestanding PMMA thin films. *Curr. Appl. Phys.* **2009**, *9*, S107–S109.

53 Huang, J.; Juszkiewicz, M.; de Jeu, W. H.; Cerda, E.; Emrick, T.; Menon, N.; Russell, T. P. Capillary wrinkling of floating thin polymer films. *Science* **2007**, *317*, 650–653.

54 O'Connell, P. A.; McKenna, G. B. Rheological measurements of the thermoviscoelastic response of ultrathin polymer films. *Science* **2005**, *307*, 1760–1763.

55 Wang, B.; Luo, D.; Li, Z.; Kwon, Y.; Wang, M.; Goo, M.; Jin, S.; Huang, M.; Shen, Y.; Shi, H.; Ding, F.; Ruoff, R. S. Camphor-enabled transfer and mechanical testing of centimeter-scale ultrathin films. *Adv. Mater.* **2018**, *30*, 1800888.

56 Bai, L.; Han, Y.; Sun, C.; An, X.; Wei, C.; Liu, W.; Xu, M.; Sun, L.; Sun, N.; Yu, M.; Zhang, H.; Wei, Q.; Xu, C.; Yang, Y.; Qin, T.; Xie, L.; Lin, J.; Huang, W. Unveiling the effects of interchain hydrogen bonds on solution gelation and mechanical properties of diarylfluorene-based semiconductor polymers. *Research* **2020,** *2020*.

57 Akabori, K. I.; Tanaka, K.; Nagamura, T.; Takahara, A.; Kajiyama, T. Molecular motion in ultrathin polystyrene films: Dynamic mechanical analysis of surface and interfacial effects. *Macromolecules* **2005**, *38*, 9735–9741.

58 Schroeder, B. C.; Chiu, Y. C.; Gu, X.; Zhou, Y.; Xu, J.; Lopez, J.; Lu, C.; Toney, M. F.; Bao, Z. Non-conjugated flexible linkers in semiconducting polymers: a pathway to improved processability without compromising device performance. *Adv. Electron. Mater.* **2016**, *2*, 1600104.

59 Siddika, S.; Balar, N.; Booth, R. E.; O'Connor, B. T. Dynamic mechanical analysis of polymer thin films using a kirigami-inspired support. *ACS Macro Lett.* **2021**, *10*, 1107–1112.

60 Shafe, A. A.; Schrickx, H. M.; Ding, K.; Ade, H.; O'Connor, B. T. Rubber-toughened organic solar cells: miscibility–morphology–performance relations. *ACS Energy Lett.* **2023**, *8*, 3720–3726.

61 Sharma, A.; Pan, X.; Campbell, J. A.; Andersson, M. R.; Lewis, D. A. Unravelling the thermomechanical properties of bulk heterojunction blends in polymer solar cells. *Macromolecules* **2017**, *50*, 3347–3354.

62 Sharma, A.; Pan, X.; Bjuggren, J. M.; Gedefaw, D.; Xu, X.; Kroon, R.; Wang, E.; Campbell, J. A.; Lewis, D. A.; Andersson, M. R. Probing the relationship between molecular structures, thermal transitions, and morphology in polymer semiconductors using a woven glass-mesh-based DMTA technique. *Chem. Mater.* **2019**, *31*, 6740–6749.

63 Feng, J.; Sun, C.; Li, S.; Ye, L. Advancing the dynamic mechanical analysis of organic semiconductor materials. *Chem. Commun.* **2024**, *60*, 10795–10804.

64 Zhang, S.; Ocheje, M. U.; Huang, L.; Galuska, L.; Cao, Z.; Luo, S.; Cheng, Y.-H.; Ehlenberg, D.; Goodman, R. B.; Zhou, D.; Liu, Y.; Chiu, Y. C.; Azoulay, J. D.; Rondeau-Gagné, S.; Gu, X. The critical role of electron-donating thiophene groups on the mechanical and thermal properties of donor–acceptor semiconducting polymers. *Adv. Electron. Mater.* **2019**, *5*, 1800899.

65 Savagatrup, S.; Makaram, A. S.; Burke, D. J.; Lipomi, D. J. Mechanical properties of conjugated polymers and polymer-fullerene composites as a function of molecular structure. *Adv. Funct. Mater.* **2014**, *24*, 1169–1181.

66 Zhang, S.; Alesadi, A.; Selivanova, M.; Cao, Z.; Qian, Z.; Luo, S.; Galuska, L.; Teh, C.; Ocheje, M. U.; Mason, G. T.; St. Onge, P. B. J.; Zhou, D.; Rondeau-Gagné, S.; Xia, W.; Gu, X. Toward the prediction and control of glass transition temperature for donor–acceptor polymers. *Adv. Funct. Mater.* **2020**, *30*, 2002221.

67 O'Connor, B.; Chan, E. P.; Chan, C.; Conrad, B. R.; Richter, L. J.; Kline, R. J.; Heeney, M.; McCulloch, I.; Soles, C. L.; DeLongchamp, D. M. Correlations between mechanical and electrical properties of polythiophenes. *ACS Nano* **2010**, *4*, 7538–7544.

68 Wang, C.; Jimison, L. H.; Goris, L.; McCulloch, I.; Heeney, M.; Ziegler, A.; Salleo, A. Microstructural origin of high mobility in high-performance poly(thieno-thiophene) thin-film transistors. *Adv. Mater.* **2010**, *22*, 697–701.

69 Andrews, E. H. Morphology and mechanical properties in semicrystalline polymers. *Pure Appl. Chem.* **1974**, *39*, 179–194.

70 Kim, T.; Kim, J. H.; Kang, T. E.; Lee, C.; Kang, H.; Shin, M.; Wang, C.; Ma, B.; Jeong, U.; Kim, T. S.; Kim, B. J. Flexible, highly efficient all-polymer solar cells. *Nat. Commun.* **2015**, *6*, 8547.

71 Kim, J. H.; Noh, J.; Choi, H.; Lee, J. Y.; Kim, T. S. Mechanical properties of polymer–fullerene bulk heterojunction films: Role of nanomorphology of composite films. *Chem. Mater.* **2017**, *29*, 3954–3961.

72 Kim, J. S.; Kim, J. H.; Lee, W.; Yu, H.; Kim, H. J.; Song, I.; Shin, M.; Oh, J. H.; Jeong, U.; Kim, T. S.; Kim, B. J. Tuning mechanical and optoelectrical properties of poly(3-hexylthiophene) through systematic regioregularity control. *Macromolecules* **2015**, *48*, 4339–4346.

73 Schrickx, H. M.; Sen, P.; Balar, N.; O'Connor, B. T. Strain alignment of conjugated polymers: method, microstructure, and applications. *Cell Rep. Phy. Sci.* **2024**, *5*, 102076.

74 Balar, N.; Rech, J. J.; Henry, R.; Ye, L.; Ade, H.; You, W.; O'Connor,

B. T. The importance of entanglements in optimizing the mechanical and electrical performance of all-polymer solar cells. *Chem. Mater.* **2019**, *31*, 5124–5132.
75 Cataldo, S.; Pignataro, B. Polymeric thin films for organic electronics: Properties and adaptive structures. *Materials* **2013**, *6*, 1159–1190.
76 De Luca, G.; Treossi, E.; Liscio, A.; Mativetsky, J. M.; Scolaro, L. M.; Palermo, V.; Samorì, P. Solvent vapour annealing of organic thin films: Controlling the self-assembly of functional systems across multiple length scales. *J. Mater. Chem.* **2010**, *20*, 2493–2498.
77 Li, W.; Hendriks, K. H.; Furlan, A.; Wienk, M. M.; Janssen, R. A. J. High quantum efficiencies in polymer solar cells at energy losses below 0.6 eV. *J. Am. Chem. Soc.* **2015**, *137*, 2231–2234.
78 Park, Y. W. Editorial for the conducting polymers for carbon electronics themed issue. *Chem. Soc. Rev.* **2010**, *39*, 2352–2353.
79 Bay, R. K.; Shimomura, S.; Liu, Y.; Ilton, M.; Crosby, A. J. Confinement effect on strain localizations in glassy polymer films. *Macromolecules* **2018**, *51*, 3647–3653.
80 Xia, W.; Keten, S. Interfacial stiffening of polymer thin films under nanoconfinement. *Extreme Mech. Lett.* **2015**, *4*, 89–95.
81 Tsui, T. Y.; Pharr, G. M. Substrate effects on nanoindentation mechanical property measurement of soft films on hard substrates. *J. Mater. Res.* **1999**, *14*, 292–301.
82 Tsui, T. Y.; McKerrow, A. J.; Vlassak, J. J. Constraint effects on thin film channel cracking behavior. *J. Mater. Res.* **2005**, *20*, 2266–2273.
83 Jia, Z.; Peng, C.; Lou, J.; Li, T. A map of competing buckling-driven failure modes of substrate-supported thin brittle films. *Thin Solid Films* **2012**, *520*, 6576–6580.
84 Guan, Q.; Laven, J.; Bouten, P. C. P.; de With, G. Mechanical failure of brittle thin films on polymers during bending by two-point rotation. *Thin Solid Films* **2016**, *611*, 107–116.
85 Torres, J. M.; Stafford, C. M.; Vogt, B. D. Elastic modulus of amorphous polymer thin films: Relationship to the glass transition temperature. *ACS Nano* **2009**, *3*, 2677–2685.
86 Kang, H.; Qian, X.; Guan, L.; Zhang, M.; Li, Q.; Wu, A.; Dong, M. Studying the adhesion force and glass transition of thin polystyrene films by atomic force microscopy. *Nanoscale Res. Lett.* **2018**, *13*, 5.
87 Müller, C. On the glass transition of polymer semiconductors and its impact on polymer solar cell stability. *Chem. Mater.* **2015**, *27*, 2740–2754.
88 Qian, Z.; Cao, Z.; Galuska, L.; Zhang, S.; Xu, J.; Gu, X. Glass transition phenomenon for conjugated polymers. *Macromol. Chem. Phys.* **2019**, *220*, 1900062.
89 Rodriquez, D.; Kim, J.-H.; Root, S. E.; Fei, Z.; Boufflet, P.; Heeney, M.; Kim, T.-S.; Lipomi, D. J. Comparison of methods for determining the mechanical properties of semiconducting polymer films for stretchable electronics. *ACS Appl. Mater. Interfaces* **2017**, *9*, 8855–8862.
90 Hasegawa, H.; Ohta, T.; Ito, K.; Yokoyama, H. Stress-strain measurement of ultra-thin polystyrene films: Film thickness and molecular weight dependence of crazing stress. *Polymer* **2017**, *123*, 179–183.
91 Zhang, S.; Ocheje, M. U.; Luo, S.; Ehlenberg, D.; Appleby, B.; Weller, D.; Zhou, D.; Rondeau-Gagné, S.; Gu, X. Probing the viscoelastic property of pseudo free-standing conjugated polymeric thin films. *Macromol. Rapid Commun.* **2018**, *39*, 1800092.
92 Zhang, S.; Wang, Y.; Mason, G. T.; Qian, Z.; Rondeau-Gagné, S.; Gu, X. Thin-film fracture behavior for diketopyrrolopyrrole semiconducting polymeric films. *Chem. Mater.* **2025**, *37*, 7804–7812.
93 Bowden, N.; Brittain, S.; Evans, A. G.; Hutchinson, J. W.; Whitesides, G. M. Spontaneous formation of ordered structures in thin films of metals supported on an elastomeric polymer. *Nature* **1998**, *393*, 146–149.
94 Alkhadra, M. A.; Root, S. E.; Hilby, K. M.; Rodriquez, D.; Sugiyama, F.; Lipomi, D. J. Quantifying the fracture behavior of brittle and ductile thin films of semiconducting polymers. *Chem. Mater.* **2017**, *29*, 10139–10149.
95 Tahk, D.; Lee, H. H.; Khang, D. Y. Elastic moduli of organic electronic materials by the buckling method. *Macromolecules* **2009**, *42*, 7079–7083.
96 Awartani, O.; Lemanski, B. I.; Ro, H. W.; Richter, L. J.; DeLongchamp, D. M.; O'Connor, B. T. Correlating stiffness, ductility, and morphology of polymer: fullerene films for solar cell applications. *Adv. Energy Mater.* **2013**, *3*, 399–406.
97 Savagatrup, S.; Chan, E.; Renteria-Garcia, S. M.; Printz, A. D.; Zaretski, A. V.; O'Connor, T. F.; Rodriquez, D.; Valle, E.; Lipomi, D. J. Plasticization of PEDOT:PSS by common additives for mechanically robust organic solar cells and wearable sensors. *Adv. Funct. Mater.* **2015**, *25*, 427–436.
98 Savagatrup, S.; Printz, A. D.; Rodriquez, D.; Lipomi, D. J. Best of both worlds: Conjugated polymers exhibiting good photovoltaic behavior and high tensile elasticity. *Macromolecules* **2014**, *47*, 1981–1992.
99 Song, R.; Schrickx, H.; Balar, N.; Siddika, S.; Sheikh, N.; O'Connor, B. T. Unveiling the stress–strain behavior of conjugated polymer thin films for stretchable device applications. *Macromolecules* **2020**, *53*, 1988–1997.
100 Paleti, S. H. K.; Haraguchi, S.; Cao, Z.; Craighero, M.; Kimpel, J.; Zeng, Z.; Sowinski, P.; Zhu, D.; Pons i Tarrés, J.; Kim, Y.; Li, Q.; Huang, J.; Kalaboukhov, A.; Mihiretie, B.; Fabiano, S.; Gu, X.; Müller, C. Benchmarking the elastic modulus of conjugated polymers with nanoindentation. *Macromolecules* **2025**, *58*, 3578–3588.
101 Kim, W.; Choi, J.; Kim, J.-H.; Kim, T.; Lee, C.; Lee, S.; Kim, M.; Kim, B. J.; Kim, T.-S. Comparative study of the mechanical properties of all-polymer and fullerene–polymer solar cells: The importance of polymer acceptors for high fracture resistance. *Chem. Mater.* **2018**, *30*, 2102–2111.
102 Oliver, W. C.; Pharr, G. M. An improved technique for determining hardness and elastic modulus using load and displacement sensing indentation experiments. *J. Mater. Res.* **1992**, *7*, 1564–1583.
103 Bruner, C.; Dauskardt, R. Role of molecular weight on the mechanical device properties of organic polymer solar cells. *Macromolecules* **2014**, *47*, 1117–1121.
104 Brand, V.; Bruner, C.; Dauskardt, R. H. Cohesion and device reliability in organic bulk heterojunction photovoltaic cells. *Sol. Energy Mater. Sol. Cells* **2012**, *99*, 182–189.
105 Balar, N.; Xiong, Y.; Ye, L.; Li, S.; Nevola, D.; Dougherty, D. B.; Hou, J.; Ade, H.; O'Connor, B. T. Role of polymer segregation on the mechanical behavior of all-polymer solar cell active layers. *ACS Appl. Mater. Interfaces* **2017**, *9*, 43886–43892.
106 Yang, Q. D.; Thouless, M. D.; Ward, S. M. Analysis of the symmetrical 90°-peel test with extensive plastic deformation. *J. Adhesion* **2000**, *72*, 115–132.
107 Fleet, E. J.; Zhang, Y.; Hayes, S. A.; Smith, P. J. Inkjet printing of self-healing polymers for enhanced composite interlaminar properties. *J. Mater. Chem. A* **2015**, *3*, 2283–2293.
108 Yue, J. K.; Liang, J.; Tan, Q. Y.; Chen, M.; Li, J. W.; Guo, Q.; Li, R. L.; Fu, Q. Scalable and high-quality monolayer graphene transfer onto polymer membranes assisted by camphor. *Chinese J. Polym. Sci.* **2024**, *42*, 1986–2001.
109 Feng, J.; Li, S.; Sun, C.; Wu, J.; Ye, L. Direct characterization of mechanical properties in fully free-standing polymeric

electronic films for stretchable devices. *Macromolecules* **2025**, *58*, 6667–6677.
110 O'Connell, P. A.; Wang, J.; Ishola, T. A.; McKenna, G. B. Exceptional property changes in ultrathin films of polycarbonate: glass temperature, rubbery stiffening, and flow. *Macromolecules* **2012**, *45*, 2453–2459.
111 Yoon, H.; McKenna, G. B. "Rubbery stiffening" and rupture behavior of freely standing nanometric thin PIB films. *Macromolecules* **2017,** *50*, 9821-9830.
112 Hopkinson, P. E.; Staniec, P. A.; Pearson, A. J.; Dunbar, A. D. F.; Wang, T.; Ryan, A. J.; Jones, R. A. L.; Lidzey, D. G.; Donald, A. M. A phase diagram of the P3HT:PCBM organic photovoltaic system: Implications for device processing and performance. *Macromolecules* **2011**, *44*, 2908–2917.
113 Wang, G.-J. N.; Molina-Lopez, F.; Zhang, H.; Xu, J.; Wu, H.-C.; Lopez, J.; Shaw, L.; Mun, J.; Zhang, Q.; Wang, S.; Ehrlich, A.; Bao, Z. Nonhalogenated solvent processable and printable high-performance polymer semiconductor enabled by isomeric nonconjugated flexible linkers. *Macromolecules* **2018**, *51*, 4976–4985.
114 Zheng, Y.; Wang, G.-J. N.; Kang, J.; Nikolka, M.; Wu, H.-C.; Tran, H.; Zhang, S.; Yan, H.; Chen, H.; Yuen, P. Y.; Mun, J.; Dauskardt, R. H.; McCulloch, I.; Tok, J. B.-H.; Gu, X.; Bao, Z. An intrinsically stretchable high-performance polymer semiconductor with low crystallinity. *Adv. Funct. Mater.* **2019**, *29*, 1905340.
115 Balar, N.; Siddika, S.; Kashani, S.; Peng, Z.; Rech, J. J.; Ye, L.; You, W.; Ade, H.; O'Connor, B. T. Role of secondary thermal relaxations in conjugated polymer film toughness. *Chem. Mater.* **2020**, *32*, 6540–6549.
116 Thapa, K.; Mooney, M.; Ma, G.; Cao, Z.; Mason, G. T.; Eedugurala, N.; Jha, S.; Patton, D. L.; Azoulay, J. D.; Rondeau-Gagné, S.; Gu, X. Deuteration effects on the physical and optoelectronic properties of donor–acceptor conjugated polymers. *Macromolecules* **2025**, *58*, 4780–4789.
117 Son, S. Y.; Samson, S.; Siddika, S.; O'Connor, B. T.; You, W. Thermocleavage of partial side chains in polythiophenes offers appreciable photovoltaic efficiency and significant morphological stability. *Chem. Mater.* **2021**, *33*, 4745–4756.
118 Yu, L.; Qian, D.; Marina, S.; Nugroho, F. A. A.; Sharma, A.; Hultmark, S.; Hofmann, A. I.; Kroon, R.; Benduhn, J.; Smilgies, D.-M.; Vandewal, K.; Andersson, M. R.; Langhammer, C.; Martín, J.; Gao, F.; Müller, C. Diffusion-limited crystallization: A rationale for the thermal stability of non-fullerene solar cells. *ACS Appl. Mater. Interfaces* **2019**, *11*, 21766–21774.
119 Pan, X.; Bjuggren, J. M.; Jevric, M.; Tan, W. L.; McNeill, C. R.; Andersson, M. R. Achieving high-efficiency organic photovoltaics from a new completely amorphous donor polymer. *Chem. Mater.* **2022**, *34*, 5103–5115.
120 Pan, X.; Andersson, M. R. Fine tuning the glass transition temperature and crystallinity by varying the thiophene-quinoxaline copolymer composition. *Materials* **2024**, *17*, 6031.
121 Han, J.; Xu, H.; Sharma, A.; Babics, M.; Bertrandie, J.; Wang, X.; Huerta Hernandez, L.; Zhang, Y.; Wen, Y.; Rosas Villalva, D.; Ramos, N.; Paleti, S. H. K.; Martin, J.; Xu, F.; Troughton, J.; Yang, R.; Gorenflot, J.; Laquai, F.; De Wolf, S.; Baran, D. In situ formation of thermoset matrices for improved stability in organic photovoltaics. *Joule* **2024**, *8*, 2883–2902.
122 Wang, Z.; Wu, Y.; Zhou, Q.; Yang, L.; Yi, Z.; Yan, Y.; Liu, Y.; Zhao, Y. Aggregation structure and glass transition of intrinsically stretchable semiconducting polymers. *Matter* **2023**, *6*, 3434–3448.
123 Balar, N.; Rech, J. J.; Siddika, S.; Song, R.; Schrickx, H. M.; Sheikh, N.; Ye, L.; Megret Bonilla, A.; Awartani, O.; Ade, H.; You, W.; O'Connor, B. T. Resolving the molecular origin of mechanical relaxations in donor–acceptor polymer semiconductors. *Adv. Funct. Mater.* **2022**, *32*, 2105597.
124 Kim, S. H.; Chung, S.; Kim, M.; Yoo, D.; Ok, E.; Kim, S.; Song, K. C.; Song, Y. J.; Kang, B.; Cho, K. Designing a length-modulated azide photocrosslinker to improve the stretchability of semiconducting polymers. *Adv. Funct. Mater.* **2023**, *33*, 2212127.
125 Kirk, B.; Pan, X.; Jevric, M.; Andersson, G.; Andersson, M. R. Introducing neat fullerenes to improve the thermal stability of slot-die coated organic solar cells. *Mater. Adv.* **2022**, *3*, 2838–2849.
126 Ocheje, M. U.; Comí, M.; Yang, R.; Chen, Z.; Liu, Y.; Yousefi, N.; Al-Hashimi, M.; Rondeau-Gagné, S. Molecular engineering of benzothiadiazole-based polymers: balancing charge transport and stretchability in organic field-effect transistors. *J. Mater. Chem. C* **2022**, *10*, 4236–4246.
127 Ghasemi, M.; Balar, N.; Peng, Z.; Hu, H.; Qin, Y.; Kim, T.; Rech, J. J.; Bidwell, M.; Mask, W.; McCulloch, I.; You, W.; Amassian, A.; Risko, C.; O'Connor, B. T.; Ade, H. A molecular interaction–diffusion framework for predicting organic solar cell stability. *Nat. Mater.* **2021**, *20*, 525–532.
128 Hultmark, S.; Paleti, S. H. K.; Harillo, A.; Marina, S.; Nugroho, F. A. A.; Liu, Y.; Ericsson, L. K. E.; Li, R.; Martín, J.; Bergqvist, J.; Langhammer, C.; Zhang, F.; Yu, L.; Campoy-Quiles, M.; Moons, E.; Baran, D.; Müller, C. Suppressing co-crystallization of halogenated non-fullerene acceptors for thermally stable ternary solar cells. *Adv. Funct. Mater.* **2020**, *30*, 2005462.
129 Siddika, S.; Peng, Z.; Balar, N.; Dong, X.; Zhong, X.; You, W.; Ade, H.; O'Connor, B. T. Molecular interactions that drive morphological and mechanical stabilities in organic solar cells. *Joule* **2023**, *7*, 1593–1608.
130 Schrickx, H. M.; Moore, C.; Shafe, A. A.; Samadani, A.; Balar, N.; Vu, D.; Rech, J. J.; You, W.; O'Connor, B. T. Discerning thermal transition behavior of conjugated polymers through in situ optical characterization of oriented films. *Chem. Mater.* **2024**, *36*, 11119–11128.
131 Huang, S. H.; Uva, A.; Upreti, S.; Sharif, A.; Fukuda, K.; Belisle, R. A.; Gu, X.; Tran, H. Reactive strand extension to improve stretchability in semiconducting polymers. *Chem. Mater.* **2025**.
132 Wang, X.; Fang, Y.; Huang, B.; Yue, Y.; Que, M.; Lan, A.; Jeong, S. Y.; Liu, K.; Liu, J.-B.; Li, L.; Woo, H. Y.; Chen, S. Flexible spacer units enhance 3D terpolymer acceptors' optoelectronic performance in rigid and flexible devices. *Macromolecules* **2025**, *58*, 3048–3057.
133 Genene, Z.; Lee, J.-W.; Lee, S.-W.; Chen, Q.; Tan, Z.; Abdulahi, B. A.; Yu, D.; Kim, T.-S.; Kim, B. J.; Wang, E. Polymer acceptors with flexible spacers afford efficient and mechanically robust all-polymer solar cells. *Adv. Mater.* **2022**, *34*, 2107361.
134 Chen, A. X.; Kleinschmidt, A. T.; Choudhary, K.; Lipomi, D. J. Beyond stretchability: Strength, toughness, and elastic range in semiconducting polymers. *Chem. Mater.* **2020**, *32*, 7582–7601.
135 Galuska, L. A.; McNutt, W. W.; Qian, Z.; Zhang, S.; Weller, D. W.; Dhakal, S.; King, E. R.; Morgan, S. E.; Azoulay, J. D.; Mei, J.; Gu, X. Impact of backbone rigidity on the thermomechanical properties of semiconducting polymers with conjugation break spacers. *Macromolecules* **2020**, *53*, 6032–6042.
136 Müller, C.; Goffri, S.; Breiby, D. W.; Andreasen, J. W.; Chanzy, H. D.; Janssen, R. A. J.; Nielsen, M. M.; Radano, C. P.; Sirringhaus, H.; Smith, P.; Stingelin-Stutzmann, N. Tough, semiconducting polyethylene-poly(3-hexylthiophene) diblock copolymers. *Adv. Funct. Mater.* **2007**, *17*, 2674–2679.
137 Lee, J. W.; Seo, S.; Lee, S. W.; Kim, G. U.; Han, S.; Phan, T. N. L.; Lee,

S.; Li, S.; Kim, T. S.; Lee, J. Y.; Kim, B. J. Intrinsically stretchable, highly efficient organic solar cells enabled by polymer donors featuring hydrogen-bonding spacers. *Adv. Mater.* **2022**, *34*, 2207544.

138 Wang, Z.; Zhang, D.; Xu, M.; Liu, J.; He, J.; Yang, L.; Li, Z.; Gao, Y.; Shao, M. Intrinsically stretchable organic solar cells with simultaneously improved mechanical robustness and morphological stability enabled by a universal crosslinking strategy. *Small* **2022**, *18*, 2201589.

139 Sun, N.; An, X.; Gong, J.; Zheng, Y.; Bai, L.; Gong, H.; Zhang, Y.; Ni, M.; Zhuo, Z.; Wei, C.; Xu, M.; Wang, J.; Han, Y.; Huang, W.; Lin, J. Intrinsically stretchable and efficient cross-linked small molecular emitter for flexible organic light-emitting diodes. *Mater. Chem. Front.* **2024**, *8*, 1950–1957.

140 Lee, J. W.; Oh, J.; Kang, W. J.; Oh, E. S.; Lee, S.; Lee, I.; Park, J.; Lee, J. Y.; Kim, T. S.; Kim, B. J. Dual-layered percolative networks of photoactive materials and elastomers for highly-stretchable, efficient organic photovoltaics with strain-induced power enhancement up to 60% strain. *Energy Environ. Sci.* **2025**, *18*, 7089–7102.

141 Liu, W.; Zhang, C.; Alessandri, R.; Diroll, B. T.; Li, Y.; Liang, H.; Fan, X.; Wang, K.; Cho, H.; Liu, Y.; Dai, Y.; Su, Q.; Li, N.; Li, S.; Wai, S.; Li, Q.; Shao, S.; Wang, L.; Xu, J.; Zhang, X.; Talapin, D. V.; de Pablo, J. J.; Wang, S. High-efficiency stretchable light-emitting polymers from thermally activated delayed fluorescence. *Nat. Mater.* **2023**, *22*, 737–745.

142 Choudhary, K.; Chen, A. X.; Pitch, G. M.; Runser, R.; Urbina, A.; Dunn, T. J.; Kodur, M.; Kleinschmidt, A. T.; Wang, B. G.; Bunch, J. A.; Fenning, D. P.; Ayzner, A. L.; Lipomi, D. J. Comparison of the mechanical properties of a conjugated polymer deposited using spin coating, interfacial spreading, solution shearing, and spray coating. *ACS Appl. Mater. Interfaces* **2021**, *13*, 51436–51446.

143 Molina-Lopez, F.; Wu, H.-C.; Wang, G.-J. N.; Yan, H.; Shaw, L.; Xu, J.; Toney, M. F.; Bao, Z. Enhancing molecular alignment and charge transport of solution-sheared semiconducting polymer films by the electrical-blade effect. *Adv. Electron. Mater.* **2018**, *4*, 1800110.

144 Shaw, L.; Hayoz, P.; Diao, Y.; Reinspach, J. A.; To, J. W. F.; Toney, M. F.; Weitz, R. T.; Bao, Z. Direct uniaxial alignment of a donor–acceptor semiconducting polymer using single-step solution shearing. *ACS Appl. Mater. Interfaces* **2016**, *8*, 9285–9296.

145 Li, G.; Zhu, R.; Yang, Y. Polymer solar cells. *Nat. Photonics* **2012**, *6*, 153–161.

146 Cao, X.; Han, Y. Control of donor–acceptor conjugated polymer crystallization for optimized film structures in organic transistors. *Polym. Sci. Technol.* **2025**, *1*, 413–435.

147 Gao, C.; Chenchai, K.; Huang, L.; Li, C.; Zhang, X.; Zhang, G.; Shao, J.; Zhang, H.; Liu, G.; Hou, Z.; Zhang, D. Polymer semiconductor blends with remarkably stable semiconducting performance under large and cyclic mechanical deformation. *Nat. Commun.* **2025**, *16*, 10388.

148 Li, X.; Ke, H.; Li, S.; Gao, M.; Li, S.; Yu, J.; Xie, H.; Zhou, K.; Zhang, K.; Ye, L. Intrinsically stretchable organic photovoltaic cells with improved mechanical durability and stability *via* dual-donor polymer blending. *Adv. Funct. Mater.* **2024**, *34*, 2400702.

149 Zhu, J.; Li, H.; Wang, H.; Gong, Y.; Li, Y.; Cheng, Y.; Hu, Y.; Xiong, J.; Wang, J.; Meng, L.; Fang, J.; Zou, W.; Wang, Y.; Liu, Y.; Yan, C.; Li, Y.; Cheng, P. Stress-dissipative strong bimodal molecular packing towards efficient and highly stretchable organic photovoltaics. *Energy Environ. Sci.* **2025**, *18*, 8171–8181.

150 Xian, K.; Zhang, K.; Zhang, T.; Zhou, K.; Zhang, Z.; Hou, J.; Zhang, H.; Geng, Y.; Ye, L. Simultaneously improving efficiency, stability and intrinsic stretchability of organic photovoltaic films *via* molecular toughening. *Energy Environ. Sci.* **2025**, *18*, 2570–2583.

151 Li, S.; Wang, Y.; Sun, C.; Feng, J.; Zuo, J.; Sun, B.; Han, D.; Gao, M.; Li, X.; Xiao, B.; Zhao, W.; Kuvondikov, V.; Nematov, S.; Jia, T.; Zhang, G.; Ye, L. A general elastomeric agent to addressing embrittlement in high-efficiency organic solar cells. *Adv. Mater.* **2026**, *38*, e16229.

152 Li, S.; Gao, M.; Zhou, K.; Li, X.; Xian, K.; Zhao, W.; Chen, Y.; He, C.; Ye, L. Achieving record-high stretchability and mechanical stability in organic photovoltaic blends with a dilute-absorber strategy. *Adv. Mater.* **2024**, *36*, 2307278.

153 Sun, B.; Li, X.; Zhao, W.; Zhang, K.; Li, S.; Sun, C.; Kuvondikov, V.; Nematov, S.; Lv, M.; Ye, L. Stress-dissipative network design unlocks stretchy all-polymer photovoltaics with record mechanical robustness. *Adv. Funct. Mater.* **2025**, *36*, e12584.

154 Ma, R.; Jiang, X.; Dela Peña, T. A.; Gao, W.; Wu, J.; Li, M.; Roth, S. V.; Müller-Buschbaum, P.; Li, G. Insulator polymer matrix construction on all-small-molecule photoactive blend towards extrapolated 15000 hour t80 stable devices. *Adv. Mater.* **2024**, *36*, 2405005.

155 Zhang, C. Y.; Liu, Y. Q.; Li, H. X.; Cui, X. Y.; Wei, Z. D.; Liu, Y. H.; Li, M. H.; Zhang, A. D.; Cheng, P.; Bo, Z. S. Stretchable all-small-molecule organic solar cells enabled by polymer elastomer confinement. *Chinese J. Polym. Sci.* **2025**, *43*, 271–277.

156 Peng, Z.; Xian, K.; Cui, Y.; Qi, Q.; Liu, J.; Xu, Y.; Chai, Y.; Yang, C.; Hou, J.; Geng, Y.; Ye, L. Thermoplastic elastomer tunes phase structure and promotes stretchability of high-efficiency organic solar cells. *Adv. Mater.* **2021**, *33*, 2106732.

157 Lee, J. W.; Nguyen, T. H. Q.; Oh, E. S.; Lee, S.; Choi, J.; Kwon, H. S.; Wang, C.; Lee, S.; Lee, J. Y.; Kim, T. S.; Kim, B. J. Establishing co-continuous network of conjugated polymers and elastomers for high-performance polymer solar cells with extreme stretchability. *Adv. Energy Mater.* **2024**, *14*, 2401191.

158 Ding, Z.; Zhang, Y.; Su, Y.; Wu, Y.; Han, Y.; Zhao, K.; Liu, S. Control of phase separation and crystallization for high-efficiency and mechanically deformable organic solar cells. *Energy Environ. Mater.* **2023**, *6*, e12421.

159 Peng, Z.; Li, S.; Zhou, K.; Zhang, Y.; Li, M.; Li, X.; Yang, C.; Bian, F.; Geng, Y.; Ye, L. Unveiling the strain-induced microstructural evolution and morphology-stretchability correlations of intrinsically stretchable organic photovoltaic films. *Adv. Energy Mater.* **2024**, *14*, 2304286.

160 Shin, E. Y.; Park, S. H.; Jeon, Y.; Kim, K.; Lee, G.; Lee, J. Y.; Son, H. J. Important role of additive in morphology of stretchable electrode for highly intrinsically stable organic photovoltaics. *ACS Appl. Energy Mater.* **2023**, *6*, 8729–8737.

161 Le, T. T.; Abbas, F.; Bourdo, S.; Watanabe, F.; Siraj, N. Counterion effects of protic ionic liquids on the conductivity and stretchability of free-standing PEDOT:PSS films. *Macromolecules* **2025**, *58*, 11718–11730.

162 Pei, L.; Han, D.; Wang, Y.; Gao, M.; Wu, J.; Sun, C.; Yu, M.; Wang, Y.-X.; Ke, H.; Li, X.; Ye, L. Advancing intrinsically stretchable organic photovoltaics with a nearly amorphous polymer semiconductor. *Adv. Funct. Mater.* **2025**, *35*, 2425892.

163 Zhu, Q.; Xue, J.; Zhang, L.; Wen, J.; Lin, B.; Naveed, H. B.; Bi, Z.; Xin, J.; Zhao, H.; Zhao, C.; Zhou, K.; Liu, S.; Ma, W. Intermolecular interaction control enables co-optimization of efficiency, deformability, mechanical and thermal stability of stretchable organic solar cells. *Small* **2021**, *17*, 2007011.

164 Zhou, K.; Xian, K.; Qi, Q.; Gao, M.; Peng, Z.; Liu, J.; Liu, Y.; Li, S.; Zhang, Y.; Geng, Y.; Ye, L. Unraveling the correlations between

mechanical properties, miscibility, and film microstructure in all-polymer photovoltaic cells. *Adv. Funct. Mater.* **2022**, *32*, 2201781.

165 Liu, J.; Qiao, J.; Zhou, K.; Wang, J.; Gui, R.; Xian, K.; Gao, M.; Yin, H.; Hao, X.; Zhou, Z.; Ye, L. An aggregation-suppressed polymer blending strategy enables high-performance organic and quantum dot hybrid solar cells. *Small* **2022**, *18*, 2201387.

166 Ma, L.; Cui, Y.; Zhang, J.; Xian, K.; Chen, Z.; Zhou, K.; Zhang, T.; Wang, W.; Yao, H.; Zhang, S.; Hao, X.; Ye, L.; Hou, J. High-efficiency and mechanically robust all-polymer organic photovoltaic cells enabled by optimized fibril network morphology. *Adv. Mater.* **2023**, *35*, 2208926.

https://doi.org/10.1007/s10118-026-3635-4